J. Fluid Mech. (1999), *vol.* 386, *pp.* 77–104. Printed in the United Kingdom

Temporal behaviour of a solute cloud in a chemically heterogeneous porous medium

By S. ATTINGER[1,2], M. DENTZ[1], H. KINZELBACH[1] AND W. KINZELBACH[2]

[1]Institut für theoretische Physik, Universität Heidelberg, Philosophenweg 19,
D-69120 Heidelberg, Germany

[2]Institut für Hydromechanik und Wasserwirtschaft, Eidgenössische Technische Hochschule Zürich,
ETH-Hönggerberg, CH-8093 Zürich, Switzerland

(Received 9 May 1997 and in revised form 5 November 1998)

In this paper we investigate the temporal behaviour of a solute cloud in a heterogeneous porous medium using a stochastic modelling approach. The behaviour of the plume evolving from a point-like instantaneous injection is characterized by the velocity of its centre-of-mass and by its dispersion as a function of time. In a stochastic approach, these quantities are expressed as appropriate averages over the ensemble of all possible realizations of the medium. We develop a general perturbation approach which allows one to calculate the various quantities in a systematic and unified way. We demonstrate this approach on a simplified aquifer model where only the retardation factor $R(\boldsymbol{x})$ due to linear instantaneous chemical adsorption varies stochastically in space. We analyse the resulting centre-of-mass velocity and two conceptually different definitions for the dispersion coefficient: the 'effective' dispersion coefficient which is derived from the average over the centred second moments of the spatial concentration distributions in every realization, and the 'ensemble' dispersion coefficient which follows from the second moment of the averaged concentration distribution. The first quantity characterizes the dispersion in a typical realization of the medium as a function of time, whereas the second one describes the (formal) dispersion properties of the ensemble as a whole. We show that for finite times the two quantities are not equivalent whereas they become identical for $t \to \infty$ and spatial dimensions $d \geqslant 2$. The ensemble dispersion coefficient which is usually evaluated in the literature considerably overestimates the dispersion typically found in one given realization of the medium. We derive for the first time explicit analytical expressions for both quantities as functions of time. From these, we identify two relevant time scales separating regimes of qualitatively and quantitatively different temporal behaviour: the shorter of the two scales is set by the advective transport of the solute cloud over one disorder correlation length, whereas the second, much larger one, is related to the dispersive spreading over the same distance. Only for times much larger than this second scale, and spatial dimensions $d \geqslant 2$, do the effective and the ensemble dispersion coefficients become equivalent due to mixing caused by the local transversal dispersion. Finally, the formalism is generalized to an extended source. With growing source size the convergence of the effective dispersion coefficient to the ensemble dispersion coefficient happens faster as the extended source already represents an ensemble of point sources. In the limit of a very large source size, convergence occurs on the time scale of advective transport over one disorder length. We derive explicit results for the temporal behaviour in the different time regimes for both point and extended sources.

1. Introduction

Flow and transport in porous media with spatial heterogeneities is investigated extensively in the literature. An example with many practically relevant implications is the transport of dissolved pollutants in the porous formations of a water-saturated aquifer. Owing to the inhomogeneities in the local flow field and to strong spatial variations of various chemical and physical system parameters, the large-scale transport properties generally are very different from those found from experiments performed on the laboratory scale. It is well established in the literature that the transport parameters characteristic of the behaviour at the field scale are dominated by the structure of the given inhomogeneities of the medium, but owing to the lack of knowledge of the detailed local structure of the soil in a given realistic setup, our predictive abilities are limited. The stochastic approach has become an invaluable tool to describe transport properties in such situations. Starting from a statistical description of the system behaviour on a local scale with a fixed time-independent structure of the inhomogeneities, the objective of the method is to derive appropriate effective quantities characteristic of the system on length and time scales larger than the laboratory scales.

The stochastic approach is well known in solid state physics and fluid mechanics where it is used to model systems with ‘quenched disorder’, see e.g. the reviews by Haus & Kehr (1987) and Bouchaud & Georges (1990). As mentioned above, the stochastic approach has also been successfully applied to various problems in groundwater hydrology. Examples can be found in the textbooks by Dagan (1989) and Gelhar (1993). The problems investigated in the present article are related to the latter context. In the generally accepted model for a heterogeneous saturated aquifer, spatial fluctuations in the hydraulic conductivity induce local random variations in the advective flow field which in turn cause a strong increase in the field-scale dispersion of a transported solute. Taking into account linear equilibrium adsorption reactions yields a retardation in transport. The influence of spatial stochastic variations in the corresponding retardation factor on the field-scale dispersion coefficient is well established in the literature, see again the discussion by Dagan (1989) and Gelhar (1993) and the references given therein. In a stochastic approach, these heterogeneities are modelled as stochastic, time-independent random fields. Characteristic field-scale transport properties then follow as appropriately defined averages over the ensemble of all possible aquifer realizations. For the case of a saturated aquifer, Gelhar & Axness (1983) followed this approach to investigate the increase of macroscopic dispersion coefficients due to spatial fluctuations in the hydraulic conductivities. Their approach has been generalized by many authors to include various effects of heterogeneities in chemical properties such as the equilibrium adsorption isotherm. A more detailed discussion of the literature is postponed to § 3.3. The properties derived by these methods describe the transport processes on asymptotically large scales. However, these methods give little information on the time scales necessary to reach this asymptotic situation. Knowledge of the transient temporal behaviour and the basic time scales involved, on the other hand, is of fundamental relevance for an adequate interpretation of field measurements and numerical simulations. The temporal behaviour of transport coefficients in a medium with spatial fluctuations in the conductivities was investigated by Dagan (1984, 1988, 1991) using a Lagrangian approach. This analysis neglects the influence of local dispersion on the transport of the solute. Dagan’s results are therefore restricted to short time scales or to situations where the initial spatial extent of the solute plume is sufficiently large to sample the medium from the beginning. Again the approach has been generalized to include other kinds of heterogeneities, see the discussion in § 3.3.

2. General concepts

In a given aquifer, the solute cloud is represented by a concentration field $c(\boldsymbol{x}, t)$. Its centre-of-mass velocity $u_j(t)$ and dispersion coefficient are given by time derivatives of the spatial moments,

$$u_j(t) = \frac{\mathrm{d}}{\mathrm{d}t}\, m_j^{(1)}(t), \tag{2.1}$$

$$D_{ij}(t) = \frac{1}{2}\frac{\mathrm{d}}{\mathrm{d}t}\, \{m_{ij}^{(2)}(t) - m_i^{(1)}(t) m_j^{(1)}(t)\}, \tag{2.2}$$

where $m_j^{(1)}(t)$, $m_{ij}^{(2)}(t)$ are the first two moments of the properly normalized spatial concentration distribution in d dimensions,

$$m_j^{(1)}(t) = \int \mathrm{d}^d x \; x_j \; p(\boldsymbol{x}, t), \tag{2.3}$$

$$m_{ij}^{(2)}(t) = \int \mathrm{d}^d x \; x_i \, x_j \; p(\boldsymbol{x}, t), \tag{2.4}$$

with a density $p(\boldsymbol{x}, t)$ given by

$$p(\boldsymbol{x}, t) = \frac{c(\boldsymbol{x}, t)}{\displaystyle\int \mathrm{d}^d y \; c(\boldsymbol{y}, t)}. \tag{2.5}$$

The time evolution of the centre-of-mass velocity $u_j(t)$ and the dispersion coefficient $D_{ij}(t)$ defined in this way depend implicitly on the spatial distribution of the heterogeneities in the given aquifer. In the stochastic modelling approach, the given heterogeneous medium is identified as one particular typical realization of a spatial stochastic process. The basic assumption of the approach is that the transport coefficients can be expressed as averages over the ensemble of all possible aquifer realizations. By construction, such averages first of all represent properties characteristic of the whole ensemble of all possible aquifer realizations. At first glance, therefore, the stochastic approach might seem to be of limited value to predict transport properties for a single given aquifer. The reason that the stochastic method also has predictive power for the individual aquifer lies in the fact that for appropriate quantities the fluctuations from realization to realization become small after the solute cloud has sampled a sufficiently large representative part of the given medium. Quantities with this property are called ‘self-averaging’. The characteristic transport properties found in different realizations of the medium in this case fluctuate only weakly around the ensemble averages constructed in the stochastic approach, so the latter indeed represent the ‘effective’ values typically found at large scales in a given heterogeneous medium.

The stochastic approach starts from quantities observable in a given realization of the medium and tries to evaluate the corresponding ensemble averages. In the present paper, we investigate the temporal behaviour of the centre-of-mass velocity and the dispersion coefficient. With respect to one single aquifer, these quantities are defined by equations (2.1) and (2.2). The corresponding averages are

$$u_j^{\mathrm{eff}}(t) \equiv \overline{u_j(t)} = \frac{\mathrm{d}}{\mathrm{d}t}\overline{m_j^{(1)}(t)}, \tag{2.6}$$

$$D_{ij}^{\mathrm{eff}}(t) \equiv \overline{D_{ij}(t)} = \frac{1}{2}\frac{\mathrm{d}}{\mathrm{d}t}\overline{\{m_{ij}^{(2)}(t) - m_i^{(1)}(t)m_j^{(1)}(t)\}}, \tag{2.7}$$

where the overbar denotes the ensemble averaging procedure. The effective dispersion coefficient given by (2.7) is different from a quantity we call the 'ensemble dispersion coefficient' D_{ij}^{ens} which reflects the dispersion characteristic of the whole ensemble of aquifer realizations. It is defined by

$$D_{ij}^{\mathrm{ens}}(t) \equiv \frac{1}{2}\,\frac{\mathrm{d}}{\mathrm{d}t}\,\{\overline{m_{ij}^{(2)}(t)} - \overline{m_i^{(1)}(t)}\;\overline{m_j^{(1)}(t)}\}. \tag{2.8}$$

The ensemble dispersion coefficient takes into account an artificial dispersion effect caused by fluctuations of the centre-of-mass positions of the solute clouds in different realizations of the inhomogeneous medium. This effect is suppressed in the effective dispersion coefficient D^{eff} as defined in (2.7), because there the centre-of-mass positions are removed before the ensemble average is performed. Generally, the experimentally observable dispersion, which is a property related to a given aquifer, is represented by the effective quantity $D_{ij}^{\mathrm{eff}}(t)$, equation (2.7). The conceptual difference between the two quantities has been well known in the literature for quite some time, see e.g. the discussion by Batchelor (1949, 1952) for the case of diffusion in turbulent flows. The corresponding definitions for static random flow fields are investigated e.g. by Rajaram & Gelhar (1993), Dagan (1990, 1991), and Kitanidis (1988).

In the literature it is often assumed that the difference between the two quantities vanishes as soon as the solute cloud has been transported over a length larger than the intrinsic correlation length of the heterogeneities. (It should, however, be mentioned that alternative views exist, such as in Kitanidis (1992) and Kapoor & Kitanidis (1996)). Therefore, usually the mathematically much simpler ensemble quantity D^{ens} is evaluated, see e.g. Kabala & Sposito (1991), Naff (1990), Shvidler (1993), Fiori (1996). For the general model of a medium with spatial fluctuations in the hydraulic conductivity as well as in the retardation factor, Bellin *et al.* (1993) generalized the Lagrangian method of Dagan (1984) to calculate the temporal behaviour of the ensemble quantity $D^{\mathrm{ens}}(t)$. More recently, Miralles-Wilhelm & Gelhar (1996) addressed the same question. The perturbation method they use again yields an approximation for the time behaviour of the ensemble dispersion coefficient $D^{\mathrm{ens}}(t)$.

As discussed above, *a priori*, one does not expect that ensemble quantities give a realistic estimate for the situation found in one typical realization of the aquifer. For comparison with an experimental situation, one should use the effective quantity $D_{ij}^{\mathrm{eff}}(t)$. In § 4, we show that for a point source at finite times for all dimensions d, the two quantities $D_{ij}^{\mathrm{eff}}(t)$ and $D_{ij}^{\mathrm{ens}}(t)$ are different not only conceptually, but also quantitatively. In § 5 we discuss the effect of an initial condition of finite extension and show that with growing initial size of the source there is a transition to the generally assumed equivalence of the two quantities also for finite times.

3. The general model

3.1. *Basic definitions*

On mesoscopic (i.e. laboratory) scales, the time evolution of a (mobile) solute in a homogeneous porous medium with instantaneous chemical adsorption is given by an advection–dispersion equation, see e.g. Dagan (1989) or Gelhar (1993),

$$\frac{\partial}{\partial t}\left(n\, c(\boldsymbol{x},t) + (1-n)\, c_{\text{ads}}(\boldsymbol{x},t)\right) + \nabla \cdot (\boldsymbol{u}_0\, c(\boldsymbol{x},t)) - \nabla \cdot \boldsymbol{D}_0 \cdot \nabla c(\boldsymbol{x},t) = 0, \qquad (3.1)$$

where $c(\boldsymbol{x},t)$ and $c_{\text{ads}}(\boldsymbol{x},t)$ are the spatial concentrations of the mobile and the adsorbed solute, respectively. Both concentrations are normalized with respect to the total volume of a representative volume element. The ratio between the accessible pore volume and the total volume of the medium is given by the effective porosity n. Here and in the following, we denote vector and tensor quantities by boldface characters. The vector $\boldsymbol{u}_0$ is the specific discharge (or 'Darcy-velocity') of the groundwater. It follows from the local permeability of the medium by Darcy's law, see e.g. Dagan (1989) or Gelhar (1993). The tensor $\boldsymbol{D}_0$ is the local bulk dispersion coefficient. Up to microscopically small corrections, it is proportional to the Darcy velocity. For a medium with linear chemical adsorption, the mobile and the adsorbed concentration are related by $c(\boldsymbol{x},t) = k_d\, c_{\text{ads}}(\boldsymbol{x},t)$ with a positive distribution coefficient k_d.

On larger scales, the various coefficients of the model become spatially inhomogeneous, and the basic equation for the time evolution of a mobile solute in a medium with linear instantaneous chemical adsorption now reads

$$R(\boldsymbol{x})\, \frac{\partial}{\partial t} c(\boldsymbol{x},t) + \nabla \cdot (\boldsymbol{u}_0(\boldsymbol{x})\, c(\boldsymbol{x},t)) + \nabla \cdot \boldsymbol{D}_0 \cdot \nabla c(\boldsymbol{x},t) = \rho(\boldsymbol{x})\delta(t). \qquad (3.2)$$

Owing to spatial fluctuations in the permeability of the porous medium, the Darcy velocity $\boldsymbol{u}_0(\boldsymbol{x})$ varies locally. As a consequence of the incompressibility of the fluid, however, one still has $\nabla \cdot \boldsymbol{u}_0(\boldsymbol{x}) = 0$. We introduced the space-dependent retardation factor $R(\boldsymbol{x}) \equiv n(\boldsymbol{x}) + (1-n(\boldsymbol{x}))\, k_d(\boldsymbol{x}) > 0$ which reflects spatial inhomogeneities in both the local porosity and the local chemical adsorption coefficient. In principle, the local dispersion tensor also varies spatially, $\boldsymbol{D}_0 = \boldsymbol{D}_0(\boldsymbol{x})$. However, as is well known in the literature, see e.g. Gelhar (1993), the related effects are negligible. In the following, we therefore assume a constant local dispersion tensor. The additional temporal δ-function multiplied with the source term $\rho(\boldsymbol{x})$ on the right-hand side represents the initial condition for an instantaneous solute injection at $t = 0$. For the mobile concentration, it implies $c(\boldsymbol{x},0) = R(0)^{-1}\rho(\boldsymbol{x})$. As boundary condition we assume a vanishing concentration at infinity.

In the stochastic approach, the particular spatial distribution of $\boldsymbol{u}_0(\boldsymbol{x})$ and $R(\mathbf{x})$ in the given system is interpreted as one single realization of a spatial stochastic process defined by the ensemble of all possible realizations. We assume this process to be ergodic, which essentially means that spatial averages can be replaced by ensemble averages. Furthermore, we assume the processes to be translation invariant in space, which in particular implies that the ensemble averages $\overline{R(\boldsymbol{x})}$ and $\overline{\boldsymbol{u}_0(\boldsymbol{x})}$ do not depend on the given position $\boldsymbol{x}$ in space. We split the spatially fluctuating fields into a deterministic and a random contribution,

$$R(\boldsymbol{x}) \equiv \overline{R}\,(1-\mu(\boldsymbol{x})) \qquad \text{and} \qquad \boldsymbol{u}_0(\boldsymbol{x}) \equiv \overline{R}\,\left(\overline{\boldsymbol{u}} - \boldsymbol{u}'(\boldsymbol{x})\right), \qquad (3.3)$$

where $\overline{R} \equiv \overline{R(\boldsymbol{x})} \geqslant 1$ is the averaged retardation factor and $\overline{\boldsymbol{u}}$ the ensemble-averaged flow velocity, normalized by $\overline{R}$ for later convenience. The fields $\mu(\boldsymbol{x})$ and $\boldsymbol{u}'(\boldsymbol{x})$ denote the normalized random fluctuation around these mean values. By construction, one has $\overline{\mu(\boldsymbol{x})} = 0$ and $\overline{\boldsymbol{u}'(\boldsymbol{x})} = 0$. The corresponding auto-correlation functions are denoted by

$$\overline{\mu(\boldsymbol{x})\,\mu(\boldsymbol{x}')} = \mathrm{C}^{\mu\mu}(\boldsymbol{x}-\boldsymbol{x}') \qquad \text{and} \qquad \overline{u_i'(\boldsymbol{x})\,u_j'(\boldsymbol{x}')} = \mathrm{C}^{uu}_{ij}(\boldsymbol{x}-\boldsymbol{x}'), \qquad (3.4)$$

where $u_i'(\boldsymbol{x})$ is the i-component of the d-dimensional field $\boldsymbol{u}'(\boldsymbol{x})$, $i = 1,\ldots,d$.

Analogously, the cross-correlation functions read

$$\overline{\mu(\boldsymbol{x})\, u_i'(\boldsymbol{x}')} = \mathrm{C}_i^{\mu u}(\boldsymbol{x} - \boldsymbol{x}'). \tag{3.5}$$

Owing to the translational invariance in space, the two-point correlation functions are functions of the distance $\boldsymbol{x} - \boldsymbol{x}'$ only. Their particular shape is to some extent arbitrary. They have to fulfil some general mathematical requirements to make the whole approach well defined; details are summarized e.g. in Gelhar (1993). Reflecting the situation in the heterogeneous medium, they should drop sharply to zero on length scales larger than an intrinsic correlation length given by the typical scale of the inhomogeneities in the medium. Note that in the framework of a second-order perturbation treatment, the transport coefficients are completely determined by the mean values $\overline{R}$, $\overline{\boldsymbol{u}}$, and the two-point correlation functions. To the given order, further details on the probability distribution of $R(\boldsymbol{x})$ and $\boldsymbol{u}_0(\boldsymbol{x})$ do not affect the transport coefficients.

If we rescale the remaining quantities in the transport equation according to

$$\mathbf{D} \equiv \mathbf{D}_0/\overline{R}, \quad g(\boldsymbol{x},t) \equiv \overline{R}\, c(\boldsymbol{x},t), \tag{3.6}$$

equation (3.2) reads

$$\frac{\partial}{\partial t} g(\boldsymbol{x},t) + \overline{\boldsymbol{u}} \cdot \nabla g(\mathbf{x},t) + \nabla \cdot \mathbf{D} \cdot \nabla g(\boldsymbol{x},t) = \rho(x)\delta(t) + \mu(\boldsymbol{x})\frac{\partial}{\partial t} g(\boldsymbol{x},t) + \boldsymbol{u}'(\boldsymbol{x}) \cdot \nabla g(\boldsymbol{x},t). \tag{3.7}$$

The (rescaled) initial condition generated by the source term on the right-hand side now reads $g(\boldsymbol{x},0) = R(0)^{-1}\overline{R}\rho(\boldsymbol{x})$. Without restriction of generality the mean flow vector $\overline{\boldsymbol{u}}$ is aligned with the 1-direction of the coordinate system,

$$\overline{\boldsymbol{u}} = \overline{u}\, \boldsymbol{e}_1 \tag{3.8}$$

where $\boldsymbol{e}_1$ is the unit vector in 1-direction, i.e. $\overline{u}_i = \overline{u}\, \delta_{i1}$ in component notation. For simplicity, and without severe restriction of generality, the local dispersion tensor $\mathbf{D}$ is assumed to be of diagonal form with a longitudinal component D_L and transversal components D_T, i.e.

$$D_{ij} = \begin{cases} D_T & \text{for} \quad i = j = 1 \\ D_L & \text{for} \quad i = j > 1 \\ 0 & \text{for} \quad i \neq j. \end{cases} \tag{3.9}$$

For the purposes of the present paper, it has some technical advantages to perform a Fourier transform with respect to the spatial variable $\boldsymbol{x}$,

$$\tilde{g}(\boldsymbol{k},t) = \int \mathrm{d}^d x\, g(\boldsymbol{x},t)\ \exp(+\mathrm{i}\boldsymbol{k}\cdot\boldsymbol{x}) \quad \text{and} \quad g(\boldsymbol{x},t) = \int_{\boldsymbol{k}} \tilde{g}(\boldsymbol{k},t)\ \exp(-\mathrm{i}\boldsymbol{k}\cdot\boldsymbol{x}) \tag{3.10}$$

where $\boldsymbol{k}$ and $\boldsymbol{x}$ are d-dimensional vectors and $\boldsymbol{k}\cdot\boldsymbol{x}$ denotes the corresponding scalar product. The Fourier-transformed functions are marked by a tilde. For the d-dimensional $\boldsymbol{k}$-integration over the whole space here and in the following we employ the shorthand notation

$$\int_{\boldsymbol{k}} \ldots \equiv \int \frac{\mathrm{d}^d k}{(2\pi)^d}\ \ldots. \tag{3.11}$$

The transport equation (3.7) then reads

$$\frac{\partial}{\partial t}\tilde{g}(\boldsymbol{k},t) + (-\mathrm{i}\boldsymbol{k}\cdot\overline{\boldsymbol{u}} + \boldsymbol{k}\cdot\mathbf{D}\cdot\boldsymbol{k})\ \tilde{g}(\boldsymbol{k},t) = \delta(t)\,\tilde{\rho}(\boldsymbol{k}) + \int_{\boldsymbol{k}'} \mathscr{L}'(\boldsymbol{k},\boldsymbol{k}';t)\,\tilde{g}(\boldsymbol{k}-\boldsymbol{k}',t) \tag{3.12}$$

with $\widetilde{\rho}(\boldsymbol{k}) = \int \mathrm{d}^d x\, \rho(\boldsymbol{x}) \exp(+\mathrm{i}\boldsymbol{k}\cdot\boldsymbol{x})$. We used the incompressibility condition $\boldsymbol{k}\cdot\widetilde{\boldsymbol{u}}'(\boldsymbol{k}) = 0$ to write the operator $\mathscr{L}'(\boldsymbol{k},\boldsymbol{k}';t)$ as

$$\mathscr{L}'(\boldsymbol{k},\boldsymbol{k}';t) \equiv \mu(\boldsymbol{k}')\frac{\partial}{\partial t} + \mathrm{i}\boldsymbol{k}\cdot\widetilde{\boldsymbol{u}}'(\boldsymbol{k}'). \tag{3.13}$$

From the definitions of the centre-of-mass velocity and the dispersion coefficient in one single realization as given by equation (2.1) and (2.2), one gets

$$u_j(t) = \frac{\mathrm{d}}{\mathrm{d}t}(-\mathrm{i}\partial_{k_j})\ \{\ln \widetilde{p}(\boldsymbol{k},t)\}|_{\boldsymbol{k}=0}, \tag{3.14}$$

$$D_{ij}(t) = \frac{1}{2}\frac{\mathrm{d}}{\mathrm{d}t}\ (-\mathrm{i}\partial_{k_i})\ (-i\partial_{k_j})\{\ln \widetilde{p}(\boldsymbol{k},t)\}|_{\boldsymbol{k}=0}, \tag{3.15}$$

where ∂_{k_i} denotes the partial derivative with respect to the $\boldsymbol{k}$-component in the i-direction, and the Fourier transform $\widetilde{p}(\boldsymbol{k},t)$ of the normalized concentration distributions (2.5) is given by

$$\widetilde{p}(\boldsymbol{k},t) = \widetilde{g}(\boldsymbol{k},t)/\widetilde{g}(\boldsymbol{k}=0,t). \tag{3.16}$$

The ensemble-averaged quantities defined by (2.6), (2.7), and (2.8) now read

$$u_j^{\mathrm{eff}}(t) = \frac{\mathrm{d}}{\mathrm{d}t}(-\mathrm{i}\partial_{k_j})\ \{\overline{\ln \widetilde{p}(\boldsymbol{k},t)}\}|_{\boldsymbol{k}=0}, \tag{3.17}$$

$$D_{ij}^{\mathrm{eff}}(t) = \frac{1}{2}\ \frac{\mathrm{d}}{\mathrm{d}t}\ (-\mathrm{i}\partial_{k_i})(-i\partial_{k_j})\{\overline{\ln \widetilde{p}(\boldsymbol{k},t)}\}|_{\boldsymbol{k}=0}, \tag{3.18}$$

$$D_{ij}^{\mathrm{ens}}(t) = \frac{1}{2}\ \frac{\mathrm{d}}{\mathrm{d}t}\ (-i\partial_{k_i})\ (-\mathrm{i}\partial_{k_j})\ \ln\{\overline{\widetilde{p}(\boldsymbol{k},t)}\}|_{\boldsymbol{k}=0}. \tag{3.19}$$

Note again the difference in the definitions for the effective and the ensemble quantities. For the first two, one has to average the logarithm of the distribution $\widetilde{p}$, whereas for the last, one first averages the distribution, and then takes the logarithm.

3.2. *Perturbation theory*

Generally, there are no closed solutions of the transport equation for given arbitrary functions $\mu(\boldsymbol{x})$, $\boldsymbol{u}'(\boldsymbol{x})$. We construct approximate solutions for the transport coefficients using a perturbation expansion with respect to these stochastic fields. One possible way to do this is to transform the transport equation into an equivalent integral equation. By iteration, the latter generates a series expansion which in our case is truncated after the second-order contributions.

In Fourier space this approach reads as follows. The Fourier-transformed transport equation (3.12) is rewritten as an integral equation,

$$\widetilde{g}(\boldsymbol{k},t) = \widetilde{g}_0(\boldsymbol{k},t)\,\widetilde{\rho}(\boldsymbol{k}) + \int_{-\infty}^{\infty} \mathrm{d}t'\ \widetilde{g}_0(\boldsymbol{k},t-t')\ \int_{\boldsymbol{k}'} \mathscr{L}'(\boldsymbol{k},\boldsymbol{k}';t')\,\widetilde{g}(\boldsymbol{k}-\boldsymbol{k}',t'). \tag{3.20}$$

The function $\widetilde{g}_0(\boldsymbol{k},t)$ solves the ‘unperturbed’ equation for the case of a point-like injection (i.e. (3.12) with $\widetilde{\rho}(\boldsymbol{k}) = 1$ and $\mathscr{L}' \equiv 0$),

$$\widetilde{g}_0(\boldsymbol{k},t) = \Theta(t)\ \exp\{-(\boldsymbol{k}\cdot\boldsymbol{D}\cdot\boldsymbol{k} - \mathrm{i}\overline{\boldsymbol{u}}\cdot\boldsymbol{k})\,t\} \tag{3.21}$$

where $\Theta(t)$ is the Heaviside step function, $\overline{\boldsymbol{u}}$ and $\boldsymbol{k}$ are d-dimensional vectors and the local dispersion coefficient $\boldsymbol{D}$ in the most general case is a d-dimensional matrix. Equation (3.20) is an implicit equation for $g(\boldsymbol{k},t)$. By iteration one generates a perturbation series in $\mathscr{L}'$ (i.e. in μ and $\boldsymbol{u}'$),

$$\begin{aligned}\tilde{g}(\boldsymbol{k},t) = \tilde{g}_0(\boldsymbol{k},t)\,\tilde{\rho}(\boldsymbol{k}) &+ \int_{\boldsymbol{k}'}\int \mathrm{d}t'\,\tilde{g}_0(\boldsymbol{k},t-t')\,\mathscr{L}'(\boldsymbol{k},\boldsymbol{k}';t')\,\tilde{g}_0(\boldsymbol{k}-\boldsymbol{k}';t')\,\tilde{\rho}(\boldsymbol{k}-\boldsymbol{k}') \\ &+ \int_{\boldsymbol{k}'\boldsymbol{k}''}\int \mathrm{d}t'\mathrm{d}t''\,\tilde{g}_0(\boldsymbol{k},t-t')\,\mathscr{L}'(\boldsymbol{k},\boldsymbol{k}';t')\,\tilde{g}_0(\boldsymbol{k}-\boldsymbol{k}',t'-t'') \\ &\times\mathscr{L}'(\boldsymbol{k}-\boldsymbol{k}',\boldsymbol{k}'';t'')\,\tilde{g}_0(\boldsymbol{k}-\boldsymbol{k}'-\boldsymbol{k}'',t'')\,\tilde{\rho}(\boldsymbol{k}-\boldsymbol{k}'-\boldsymbol{k}'')\ +\cdots. \end{aligned} \tag{3.22}$$

This series, truncated after the second order in $\mathscr{L}'$, constitutes the basis of the perturbational treatment of the transport parameters. It defines a series expansion with respect to the strength of the fluctuation operator $\mathscr{L}'$.

3.3. *Disorder-induced contributions to the transport coefficients*

To calculate transport parameters such as the effective velocity $u_j^{\mathrm{eff}}(t)$, the effective dispersion coefficient $D_{ij}^{\mathrm{eff}}(t)$, and the ensemble dispersion coefficient $D_{ij}^{\mathrm{ens}}(t)$, one inserts the perturbation series (3.22) into the corresponding definitions (3.17) to (3.19), and expands the resulting expressions again consistently up to second order in $\mathscr{L}'$. Finally, one performs the appropriate ensemble averages using the disorder correlation functions (3.4) and (3.5). One ends up with explicit integral expressions for the quantities under consideration. All contributions linear in $\mathscr{L}'$ drop out after performing the averages since the random fields involved have zero mean by construction. So to second-order perturbation theory, the resulting expression for some arbitrary quantity X is of the form $X = X_{\mathrm{local}} + \delta^{\mu\mu}\{X\} + \delta^{uu}\{X\} + \delta^{\mu u}\{X\}$, where X_{local} is the local (or laboratory scale) value of the quantity which follows from the transport equation if all spatial fluctuations are suppressed. The non-vanishing second-order contributions denoted by $\delta^{\mu\mu}\{X\}$, $\delta^{uu}\{X\}$, and $\delta^{\mu u}\{X\}$ modify the 'bare' local value, reflecting the influence of the spatial inhomogeneities. They contain the correlation functions (3.4) and (3.5), $C^{\mu\mu}$, C^{uu}, and $C^{\mu u}$, respectively, as linear integral kernels. The physical origin of these contributions, therefore, can be traced back to fluctuations in the retardation factor, to fluctuations in the flow field, and to the cross-correlations between these two kinds of inhomogeneities, respectively. In the final second-order result, they simply add up. The centre-of-mass velocity and the two different dispersion coefficients read

$$u_j^{\mathrm{eff}}(t) = u_j + \delta^{\mu\mu}\{u_j^{\mathrm{eff}}\}(t) + \delta^{uu}\{u_j^{\mathrm{eff}}\}(t) + \delta^{\mu u}\{u_j^{\mathrm{eff}}\}(t), \tag{3.23}$$

$$D_{ij}^{\mathrm{eff}}(t) = D_{ij} + \delta^{\mu\mu}\{D_{ij}^{\mathrm{eff}}\}(t) + \delta^{uu}\{D_{ij}^{\mathrm{eff}}\}(t) + \delta^{\mu u}\{D_{ij}^{\mathrm{eff}}\}(t), \tag{3.24}$$

$$D_{ij}^{\mathrm{ens}}(t) = D_{ij} + \delta^{\mu\mu}\{D_{ij}^{\mathrm{ens}}\}(t) + \delta^{uu}\{D_{ij}^{\mathrm{ens}}\}(t) + \delta^{\mu u}\{D_{ij}^{\mathrm{ens}}\}(t). \tag{3.25}$$

As is established in the literature, on the field scale the various contributions can be of the same order of magnitude, see e.g. Bellin *et al.* (1993).

Using the above notation, the existing literature can be classified according to the various limits and contributions which are investigated. Starting from a slightly different but equivalent perturbation theory setup, Gelhar & Axness (1983) calculated the infinite time limit of the corrections due to spatial fluctuations in the flow field. Their approach yields ensemble quantities only: their main focus lies in the asymptotic quantity $\lim_{t\to\infty}\delta^{uu}\{D_{ij}^{\mathrm{ens}}\}(t) = \delta^{uu}\{D_{ij}^{\mathrm{ens}}\}(\infty)$. The approach has been generalized to include the contributions $\delta^{\mu\mu}\{D_{ij}^{\mathrm{ens}}\}(\infty)$ and $\delta^{\mu u}\{D_{ij}^{\mathrm{ens}}\}(\infty)$ due to retardation fluctuations later on, see e.g. Garabedian, Gelhar & Celia (1988) and Gelhar (1993), where the various asymptotic results are summarized and the corresponding original literature is discussed. Dagan (1990, 1991) analysed the infinite time limit of the effective and of the ensemble corrections due to spatial fluctuations in the flow field, $\delta^{uu}\{D_{ij}^{\mathrm{eff}}\}(\infty)$ and $\delta^{uu}\{D_{ij}^{\mathrm{ens}}\}(\infty)$, in a Lagrangian framework, neglecting the influence of the local dispersion (i.e. $\boldsymbol{D}_0 \equiv 0$ in (3.2)); Rajaram & Gelhar (1993) re-derived the equivalent results in an Eulerian context. For the case of a point-like injection both approaches find $\delta^{uu}\{D_{ij}^{\mathrm{ens}}\}(\infty) > 0$, whereas the corresponding effective quantity is given by $\delta^{uu}\{D_{ij}^{\mathrm{eff}}\}(\infty) = 0$. The result illustrates clearly that, in general, ensemble and effective quantities indeed are not equivalent. In the case of an initial concentration distribution of a finite size, the same approach yields an effective coefficient $D_{ij}^{\mathrm{eff}}(\infty)$ which depends on the transversal width of the initial plume, whereas the corresponding asymptotic ensemble quantity is completely independent of the initial condition. Note, however, that the situation becomes different if the effect of the local transversal dispersion is included. As is discussed in detail below, owing to transversal dispersive mixing, one now finds $D_{ij}^{\mathrm{eff}}(\infty) = D_{ij}^{\mathrm{ens}}(\infty) > 0$, a result already suggested qualitatively by Dagan in the conclusions of his 1991 paper. In Metzger, Kinzelbach & Kinzelbach (1996) the infinite time limit of the effective and of the ensemble corrections $\delta^{\mu\mu}\{D_{ij}^{\mathrm{eff}}\}(\infty)$ and $\delta^{\mu\mu}\{D_{ij}^{\mathrm{ens}}\}(\infty)$, due to spatial fluctuations in the retardation factor, are investigated by a perturbational treatment similar to the one given in the previous section.

The asymptotic results describe the transport on the field scale, but give no information on the time scales necessary to reach this asymptotic situation. The problem of the temporal behaviour of the transport parameters was first addressed by Dagan (1984) and (1988), using a second-order treatment in a Lagrangian framework, neglecting the influence of the local dispersion (i.e. $\boldsymbol{D}_0 \equiv 0$ in (3.2)). In our notation, this approach yields $\delta^{uu}\{D_{ij}^{\mathrm{ens}}\}$ for vanishing local dispersion. Naff (1990) derived similar results from a perturbation treatment of the transport equation; Shvidler (1993) investigated the same quantity using an operator method in a second-order approximation. The transient behaviour of the ensemble contributions due to spatial fluctuations in the retardation factor is derived by Chrysikopoulos, Kitanidis & Roberts (1990) for a one-dimensional model. Bellin *et al.* (1993) generalize the approach of Dagan (1984) to a chemically heterogeneous medium and calculate the ensemble quantities $\delta^{\mu\mu}\{D_{ij}^{\mathrm{ens}}\}(t)$ and $\delta^{\mu u}\{D_{ij}^{\mathrm{ens}}\}(t)$. Finally, most recently, Miralles-Wilhelm & Gelhar (1996) gave perturbation theory expressions for the ensemble quantities $\delta^{\mu\mu}\{D_{ij}^{\mathrm{ens}}\}(t)$, $\delta^{uu}\{D_{ij}^{\mathrm{ens}}\}(t)$, and $\delta^{\mu u}\{D_{ij}^{\mathrm{ens}}\}(t)$ starting from the transport equation.

In the perturbation theory formulation introduced above, all heterogeneity-induced contributions to the transport coefficients as given in equation (3.23) can be evaluated systematically and in a unified way for arbitrary times. The technical details of the calculations, however, are somewhat tedious and not particularly illustrative. For the present paper, therefore we decided to restrict the discussion to the contributions due to the random spatial fluctuations in the retardation coefficient, i.e. to $\delta^{\mu\mu}\{u_j^{\mathrm{eff}}\}(t)$, $\delta^{\mu\mu}\{D_{ij}^{\mathrm{eff}}\}(t)$, and $\delta^{\mu\mu}\{D_{ij}^{\mathrm{ens}}\}(t)$. In the simplified model used by Chrysikopoulos *et al.* (1990) and Metzger *et al.* (1996), where only the retardation factor varies locally, whereas the flow field remains constant, these are the only disorder contributions. This kind of simplified model might be appropriate to describe the transport of an organic solute in an aquifer, which is comparatively homogeneous with respect to the hydraulic conductivity, but exhibits a strongly varying organic carbon content which determines the retardation factor, see Karickhoff, Brown & Scott (1979). In general, however, the contributions due to the spatial inhomogeneities in the retardation factor will hardly ever show up as an isolated effect in a realistic aquifer situation. Nevertheless, the corresponding simplified model is an extremely useful starting point to introduce the basic concepts, mathematical tools, generic results, and interpretations of various time regimes and properties: the resulting integral expressions are complex enough to show generic features which remain unchanged in more complicated situations, while at the same time they are simple enough to serve as an introduction to the techniques involved.

The δ^{uu} and $\delta^{\mu u}$ contributions in (3.23) which are ignored in the present paper have been evaluated by Dentz (1997) and Dentz *et al.* (1998) using methods analogous to those described here. Owing to the large number of terms involved, the calculation is technically less transparent. As a remarkable fact, however, we found that the qualitative features and interpretations derived in the present paper for the simplified model remain completely unchanged in the general case.

4. Spatially heterogeneous retardation factor: explicit results for a point-like initial condition

In this section, we concentrate on contributions due to spatial fluctuations in the retardation factor. In the corresponding simplified model the only disorder-induced corrections to the transport coefficients are given by $\delta^{\mu\mu}\{u_j^{\text{eff}}\}(t)$, $\delta^{\mu\mu}\{D_{ij}^{\text{eff}}\}(t)$, and $\delta^{\mu\mu}\left\{D_{ij}^{\text{ens}}\right\}(t)$. So for this model, where $\boldsymbol{u}'(\boldsymbol{x}) \equiv 0$ in (3.7), one has

$$u_i^{\text{eff}}(t) = \overline{u}_i + \delta^{\mu\mu}\{u_i^{\text{eff}}\}(t), \tag{4.1}$$

$$D_{ij}^{\text{eff}}(t) = D_{ij} + \delta^{\mu\mu}\{D_{ij}^{\text{eff}}\}(t), \tag{4.2}$$

$$D_{ij}^{\text{ens}}(t) = D_{ij} + \delta^{\mu\mu}\{D_{ij}^{\text{ens}}\}(t). \tag{4.3}$$

In the following, we derive analytical results for these quantities for the case of a point-like injection of tracer at time $t = 0$. This initial condition might appear somewhat artificial since in a realistic field situation the source always has some finite spatial extent. It is, however, a quite appropriate starting point to isolate and understand the basic mechanisms governing the temporal behaviour of the transport model. The extension of the analysis to the case of initial conditions with a finite spatial extent is given in § 5.

4.1. *Results for an isotropic field situation*

A point-like injection of tracer is described by a spatial δ-function as source term in equation (3.7),

$$\rho(\boldsymbol{x}) = \delta^d(\boldsymbol{x}). \tag{4.4}$$

To derive explicit results, we have to specify the spatial correlation function. As discussed in § 3.1, the specific form of the spatial correlation function $\overline{\mu(\boldsymbol{x})\mu(\boldsymbol{x}')} = C^{\mu\mu}(\boldsymbol{x}-\boldsymbol{x}')$ is to some extent arbitrary. One convenient choice used in the literature which captures the required general properties in a qualitatively satisfying way is a Gauss-shaped correlation function,

$$C^{\mu\mu}(\boldsymbol{x}) = q_0 \, \exp\left(-\boldsymbol{x}^2/\,2\, l_0^2\right) \tag{4.5}$$

with correlation length l_0. In d dimensions this implies a Fourier spectrum $\widetilde{C}^{\mu\mu}(\boldsymbol{k}) = \int \mathrm{d}^d x \, C^{\mu\mu}(\boldsymbol{x}) \, \exp(\mathrm{i}\boldsymbol{k}\cdot\boldsymbol{x})$ of the form

$$\widetilde{C}^{\mu\mu}(\boldsymbol{k}) = q_0 \left(2\pi l_0^2\right)^{d/2} \, \exp\left(-\boldsymbol{k}^2\, l_0^2/2\right). \tag{4.6}$$

From definition (3.3), one easily verifies that the constant q_0 is proportional to the variance σ_{RR}^2 of the retardation factor,

$$q_0 = \frac{\overline{R^2} - \overline{R}^2}{\overline{R}^2} = \frac{\sigma_{RR}^2}{\overline{R}^2}. \tag{4.7}$$

It specifies the typical strength of local fluctuations in the retardation factor.

In the case of an isotropic local dispersion tensor, i.e. for

$$D_L = D_T \equiv D \tag{4.8}$$

in (3.9), and a Gauss-shaped correlation function as given above, more or less all of the integrations in the perturbation theory expressions can be performed explicitly. For $d = 3$ (more generally: for odd dimensions) one is in the lucky situation that the expressions can be reduced to combinations of standard functions. This makes it possible to study the temporal behaviour of $u_j^{\text{eff}}(t)$, $D_{ij}^{\text{eff}}(t)$, and $D_{ij}^{\text{ens}}(t)$ in full detail. The results are listed in Appendix B for completeness and further reference. Here in the main text we concentrate on the most important characteristic features of these solutions.

From the explicit calculations sketched in the Appendix, one identifies two independent time scales, τ_u and τ_D, given by

$$\tau_u \equiv l_0/\overline{u} \quad \text{and} \quad \tau_D \equiv l_0^2/D \tag{4.9}$$

which play a crucial role in the discussion of various time regimes below. Both scales have a direct physical interpretation: in the time given by τ_u the solute is advectively transported over the distance of one disorder correlation length l_0; in the time τ_D, on the other hand, the solute cloud has spread by local dispersion over the same length. The ratio between these scales is denoted by ϵ in the following (note that ϵ is the inverse of the microscopic Péclet number Pe):

$$\epsilon \equiv \frac{\tau_u}{\tau_D} = \frac{D}{\overline{u}\, l_0} = \frac{1}{Pe}. \tag{4.10}$$

In a realistic soil situation, one has $\epsilon \ll 1$, see e.g. Roberts, Goltz & Mackay (1986) or Gelhar (1993), so the two time scales are clearly separated,

$$\tau_u \ll \tau_D. \tag{4.11}$$

Note especially that for times $t \ll \tau_u$ all ensemble-averaged quantities have only a restricted formal meaning with respect to properties found in a given aquifer realization. For times $t \ll \tau_u$ the solute cloud (which starts from a point-like injection at $t = 0$) has travelled a distance much shorter than the correlation length l_0 of the inhomogeneities in the aquifer. It has spread due to the local dispersion, but for the given times the resulting width is again extremely small compared to l_0. For a travelling particle in a given aquifer the whole situation looks like that of a homogeneous medium, but of course there are large differences from one realization of the medium to the other, contributing to the ensemble average of each fluctuating quantity in this time regime.

4.1.1. *Centre-of-mass velocity*

As introduced above, the constant pore-scale velocity vector points in the 1-direction. By symmetry, the corresponding averaged centre-of-mass velocity of the solute cloud is also aligned along this direction, i.e. one has

$$u_j^{\mathrm{eff}}(t) = u^{\mathrm{eff}}(t)\,\delta_{j1}, \tag{4.12}$$

where $u^{\mathrm{eff}}(t)$ is a scalar function. Let us first re-investigate its long-time limit $t \to \infty$. The perturbative solution given in Appendix B consists of combinations of error-functions and Gaussians. Since the asymptotic behaviour of these functions is well known, cf. Abramowitz & Stegun (1972), it is easy to extract the asymptotic long-time behaviour from these results. For all spatial dimensions, the effective centre-of-mass velocity remains unchanged in this limit,

$$\lim_{t\to\infty} u^{\mathrm{eff}}(t) = \overline{u} = u_0 / \overline{R} \tag{4.13}$$

in agreement with Bellin *et al.* (1993) and Metzger, Kinzelbach & Kinzelbach (1996). It is possible to show that this result actually is exact beyond low-order perturbation theory. The higher orders of the perturbation expansion vanish in the limit $t \to \infty$, cf. Attinger (1997).

In passing, we note that for the opposite limit $t \to 0$, one finds the exact result $u^{\mathrm{eff}}(t=0) = u_0\,\overline{R(\boldsymbol{x})^{-1}}$ by a simple non-perturbative argument, cf. Attinger (1997), which is consistent with the expression derived by second-order perturbation theory. This $t \to 0$ behaviour agrees with results derived by Kabala & Sposito (1991). Their approximation (a temporal cumulant expansion), however, breaks down for larger times, so it does not reflect the cross-over to the asymptotic long time limit given above. The cross-over behaviour of the centre-of-mass velocity, being proportional to $\overline{R^{-1}}$ for small times, and proportional to $\left(\overline{R}\right)^{-1}$ for large times, has also been observed in numerical simulations, see Burr, Sudicky & Naff (1994).

The full perturbation theory result which follows from Appendix B shows that $u^{\mathrm{eff}}(t)$ in $d=3$ is a monotonically decreasing function of time. On the time scale τ_u it has almost reached its final asymptotic value u, but there are minor corrections of the order of the local (microscopic) dispersion coefficient D which eventually die out completely for times $t \gg \tau_u$. In a realistic soil situation, where, as mentioned before, one has $\epsilon = D/\overline{u}\,l_0 \ll 1$ these corrections are quantitatively negligible. The spread induced by the local dispersion, however, plays a crucial role to smooth out sample to sample fluctuations. The local dispersion is the basic physical mechanism to make sure that the formal ensemble average also acquires a meaning for a given realization of the medium. This point is discussed in detail in the following subsection in connection with the dispersion coefficient, where this role becomes apparent in a more dramatic fashion.

4.1.2. *Dispersion*

A more interesting behaviour is found for the temporal evolution of the dispersion coefficients. In the following discussion, we shall mainly concentrate on the *longitudinal* components of the dispersion tensor corresponding to the direction of advective transport, $D_{11}^{\mathrm{eff}}(t)$ and $D_{11}^{\mathrm{ens}}(t)$. The heterogeneities of the medium change the behaviour of these coefficients in a quantitatively relevant way, whereas the corresponding transversal parts are only weakly influenced by the stochastic fluctuations of the retardation factor. The lengthy explicit expressions for their complete temporal behaviour follow from Appendix B. In the long time limit $t \to \infty$, the transversal dispersion coefficient reduces to the initial pore-scale dispersion coefficient D; all deviations from this value for shorter times are also of the order of this pore-scale dispersion coefficient, i.e. microscopically small. Larger temporal variations are found for the *longitudinal* dispersion coefficients $D_{11}^{\mathrm{eff}}(t)$ and $D_{11}^{\mathrm{ens}}(t)$. Again the full results are derived from the explicit perturbative expressions of Appendix B. They consist of various combinations of error-functions and Gaussians with well known asymptotic properties given e.g. in Abramowitz & Stegun (1972).

In the asymptotic limit $t \to \infty$, the expression for the three-dimensional ($d = 3$) longitudinal dispersion coefficient reads

$$\delta^{\mu\mu}\{D_{11}^{\mathrm{eff}}\}(\infty) = \delta^{\mu\mu}\{D_{11}^{\mathrm{ens}}\}(\infty) = (\pi/2)^{1/2} q_0 \,\bar{u}\, l_0\{1 - \exp(1/2\epsilon^2)\,\mathrm{erfc}\,((2\epsilon^2)^{-1/2})\}. \quad (4.14)$$

Again, similarly to the asymptotic results discussed in the previous subsection, these expressions can be shown to be exact. The higher-order corrections of the perturbation series vanish in the limit $t \to \infty$, Attinger (1997).

The particular form of (4.14) reflects the special choice of a Gaussian for the disorder correlation function. Similar results for box-shaped and exponential correlation functions are given in Metzger *et al.* (1996, 1998). In the practically most relevant case of small $\epsilon \ll 1$ the common feature of these results is that their leading part is proportional to $\bar{u}l_0$. It can be shown that this is generally true for arbitrary correlation functions which decay sufficiently fast for large distances, see Attinger (1997).

From the asymptotic long-time results, one might tend to conclude that the conceptual difference between D^{ens} and D^{eff} stressed in § 2 is completely irrelevant for all practical situations: For dimensions $d \geqslant 2$ the difference between the two quantities vanishes and it is sufficient to evaluate the mathematically simpler ensemble quantity D^{ens}. However, as figure 1 shows, this conclusion turns out to be wrong as soon as one investigates the full temporal behaviour of these quantities. The figure shows a plot for $D_{11}^{\mathrm{eff}}(t)$ and $D_{11}^{\mathrm{ens}}(t)$ as a function of time t for the case $d = 3$. We plotted the full perturbation theory results for these quantities as they follow from the expressions given in Appendix B. The same data are given as a logarithmic plot in figure 1(*a*), and as a linear plot in 1(*b*), since both scalings stress different characteristic features in the various time regimes.

In the figure, as well as in the explicit results given in Appendix B, the two relevant time scales $\tau_u \equiv l_0/\bar{u}$ and $\tau_D \equiv l_0^2/D$ introduced in equation (4.9) are identified. As discussed there, $\epsilon \equiv \tau_u/\tau_D \ll 1$, i.e. the scales are well separated. As figure 1 shows, for times $t \gg \tau_D$, i.e. in the limit $t \to \infty$, the difference between D^{eff} and D^{ens} vanishes as discussed before, but this asymptotic result is reached for extremely large times only. For smaller times, there is a large difference between the two quantities. The mathematically simpler ensemble dispersion coefficient D^{ens} which is generally favoured in the literature, overestimates the preasymptotic dispersion in a typical realization of the medium considerably. The time scales τ_u and τ_D separate three different time-regimes:

Short-time regime: $t \ll \tau_u$

During times smaller than τ_u, the solute cloud has only reached a region in space smaller than one disorder correlation length. For the travelling particles in a given realization of the medium, the world seems homogeneous. But of course there are large differences from one realization of the medium to the next. In the given time regime, therefore, the stochastic ensemble approach has no predictive power at all with respect to the given 'real' aquifer. The behaviour of the solute depends on the local details of this aquifer. So in this sense, D^{eff} as well as D^{ens} have only a formal meaning. A simple non-perturbative argument shows that for $t = 0$, the two quantities coincide, cf. Attinger (1997). Similarly to the behaviour of the centre-of-mass velocity discussed in the previous subsection, one gets $D_{11}^{\mathrm{eff}}(t = 0) = D_{11}^{\mathrm{ens}}(t = 0) = D_0\,\overline{R(\boldsymbol{x})^{-1}}$,

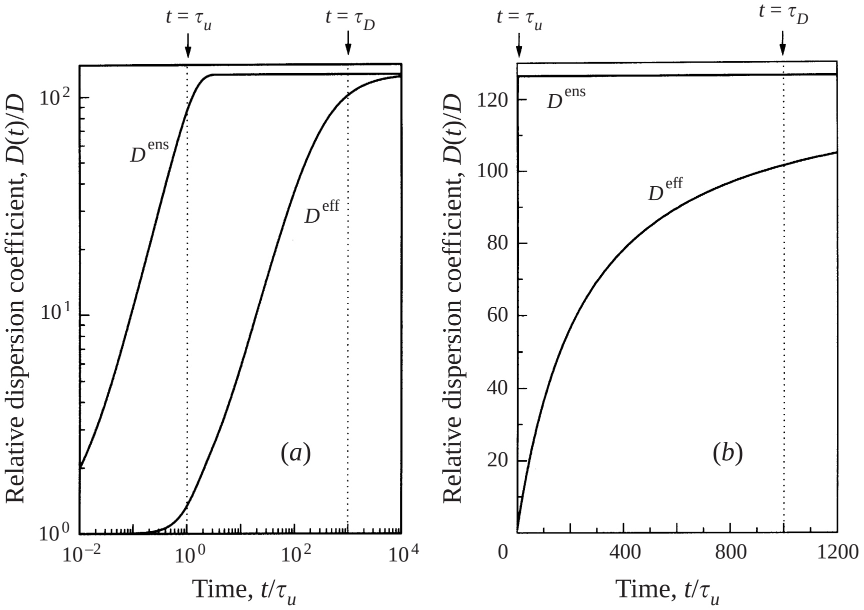

FIGURE 1. Effective and ensemble dispersion coefficients in $d = 3$ as a function of time for a point-like initial condition (with $\epsilon = \tau_u/\tau_D = 10^{-3}$ and $q_0 = 10^{-1}$): (*a*) logarithmic plot; (*b*) linear plot.

consistent with the perturbation theory result to second order in μ. The result for $t \to 0$ agrees with the corresponding expressions of Bellin *et al.* (1993). With increasing time, the two quantities $D_{11}^{\text{eff}}(t)$ and $D_{11}^{\text{ens}}(t)$ show a different time evolution. In the short-time regime, the effective quantity $D_{11}^{\text{eff}}(t)$ remains of the order of the original small microscopic initial value, whereas the ensemble quantity $D_{11}^{\text{ens}}(t)$ for times t of the order of the advective time scale τ_u has almost reached the final asymptotic long-time value.

Intermediate time-regime: $\tau_u \ll t \ll \tau_D$

In the intermediate time regime, the ensemble quantity $D_{11}^{\text{ens}}(t)$ has more or less reached its final long-time value $D_{11}^{\text{ens}}(\infty)$ given above. It approaches this macroscopic value exponentially fast on the τ_u-scale. A more careful investigation of the closed results shows that actually during the whole time regime under consideration $D_{11}^{\text{ens}}(t)$ still increases slightly, but this increase is of the order of the initial microscopic dispersion coefficient, so compared to the large value already reached at the beginning of the regime, these changes are negligible (and more or less invisible in the figure).

The behaviour of the effective quantity $D_{11}^{\text{eff}}(t)$ is completely different. In the time-regime under consideration, $D_{11}^{\text{eff}}(t)$ grows from a (microscopically) small value for times $t \approx \tau_u$ to the macroscopic asymptotic value. For times small compared to the dispersive time scale, $t \ll \tau_D$, there is a linear increase in $D_{11}^{\text{eff}}(t)$. For larger times, the curve bends to approach the final long-time value. Note that even at times of the order of the dispersive time scale τ_D the effective dispersion coefficient still has not reached its final asymptotic long-time value.

Long-time regime: $t \gg \tau_D$

For times $t \gg \tau_D$, the effective dispersion coefficient also reaches the final asymptotic value. The approach to this value is quite slow, given by an inverse power law

$\propto \left(t/\tau_D\right)^{-(d-1)/2}$ which depends on the space dimension d, see § 4.2. To reach a qualitative interpretation of these results, it is useful to reconsider the most important differences between the two averaging prescriptions used to define $D_{11}^{\mathrm{eff}}(t)$ and $D_{11}^{\mathrm{ens}}(t)$. We start from a point-like injection of solute at time $t = 0$ and try to derive predictions for the dispersion as a function of time representative for a given ('real') aquifer. As discussed in the introduction, this information is encoded in the effective dispersion coefficient $D_{11}^{\mathrm{eff}}(t)$ as defined by equation (2.7). This quantity is conceptually different from the ensemble dispersion coefficient $D_{11}^{\mathrm{ens}}(t)$, equation (2.8), which includes further effects resulting from large fluctuations between various realizations of the medium. This is most clearly illustrated if one considers a (hypothetical) situation where there is no microscopic dispersion at all. Starting from a point-like injection, the solute cloud in a given aquifer does not spread at all. Owing to the fluctuations in the retardation factor, it moves slower or faster, depending on the particular value of $R(\boldsymbol{x})$ at the given position in space, but its width remains zero for all times since there is no physical mechanism to spread out the solute cloud. This is correctly reflected by the fact that for this situation the effective dispersion remains zero for all times,

$$D_{11}^{\mathrm{eff}}(t)\,\big|_{D=0} \equiv 0. \tag{4.15}$$

The ensemble dispersion coefficient, on the other hand, even in this hypothetical case shows a non-trivial time behaviour more or less identical to the one plotted in figure 1. The explicit result derived from the perturbation theory expression given in Appendix B reads

$$D_{11}^{\mathrm{ens}}(t)\,\big|_{D=0} = (\pi/2)^{1/2}\, q_0\, l_0\, \bar{u}\, \mathrm{erf}\,(2^{-1/2}\; t/\tau_u), \tag{4.16}$$

where $\mathrm{erf}(z)$ denotes the error function as defined in Abramowitz & Stegun (1972). For times $t \gg \tau_u$ it reaches the macroscopic value $D_{11}^{\mathrm{ens}}(\infty) = (\pi/2)^{1/2}\; q_0\, l_0\, \bar{u}$. This behaviour is due to the fact that there are large sample to sample fluctuations in the centre-of-mass position of the concentration distribution which are included in the ensemble-averaging procedure used to define D_{11}^{ens}. These fluctuations show up as an artificial, purely advective nonphysical dispersion effect. The whole result is independent of the spatial dimension – which is no surprise since in the case without local dispersion the system behaves effectively one-dimensionally in any dimension: lacking the basic physical mechanism, there is no mass exchange into the transversal directions. In some sense, the ensemble quantity yields a 'worst case' estimate which is interesting for risk assessment studies, but which does not reflect the typical behaviour in a given aquifer for real mixing.

The same observation for the situation of a vanishing local dispersion is discussed in Dagan (1991) for the case of the dispersion contributions due to spatial fluctuations of the flow field. As already indicated there, the basic mechanism necessary for D_{11}^{eff} to reach the macroscopic asymptotic value is the diffusive spreading into directions *transversal* to the advective flow. As soon as one considers a more general model with non-isotropic pore-scale dispersion, i.e. for $D_L \neq D_T$ in the tensor (3.9), the relevant dispersive time scale therefore should be set by the *transversal* part D_T of the microscopic dispersion coefficient. This is confirmed by the investigations presented in § 4.2.

The explicit solution for the time behaviour as plotted in figure 1 shows that the relevant time scale to reach the asymptotic situation is given by τ_D. For times $t \gg \tau_D$ the solute cloud has broadened diffusively over a region larger than the typical scale l_0 set by the correlation length of the inhomogeneous medium. In the (hypothetical) dispersion-free case discussed above, the time scale τ_D is infinite, D_{11}^{eff} therefore never reaches a macroscopically large asymptotic value.

4.2. *Generalization to anisotropic field situations*

In the interpretation put forward in §4.1.2, we identified the transversal pore-scale dispersion as the basic mechanism which sets the time scale where the macroscopic asymptotic value of the dispersion coefficient is reached in a given realization of the medium. The explicit calculations, however, for technical reasons were restricted to the case of an isotropic pore-scale dispersion tensor, i.e. $D_T = D_L = D$ in (3.9). The different roles of D_L and D_T, therefore, did not show up explicitly in the results. For the more general case $D_T \neq D_L$ the integral expressions collected in Appendix A, equations (A 9) to (A 11) are no longer reducible to standard functions. But in the practically most interesting case of small pore-scale dispersion, however, it is actually possible to extract the leading behaviour for any dimension d for small values of the pore-scale dispersion coefficients. We assume $D_L \gg D_T$ which is the case in realistic field situations, see e.g. Gelhar (1993). The different micro-dispersion coefficients generate two instead of one dispersion time scales,

$$\tau_{D_L} = l_0^2 \,/\, D_L \quad \text{and} \quad \tau_{D_T} = l_0^2 \,/\, D_T. \tag{4.17}$$

In analogy to the isotropic situation we assume

$$\tau_u \ll \tau_{D_L} \ll \tau_{D_T} \qquad \text{and} \qquad \epsilon_T \equiv \tau_u/\tau_{D_T} \ll \epsilon_L \equiv \tau_u/\tau_{D_L} \ll 1. \tag{4.18}$$

The Fourier-integrations in the explicit perturbation theory expressions of Appendix A, equations (A 9) to (A 11), can again be performed explicitly yielding (C 1) to (C 3) in Appendix C. Owing to the Gaussian structure of the disorder correlation function $C^{\mu\mu}$ the integrals factorize into a product of one longitudinal and $(d-1)$ transversal factors. The approximations are discussed in Appendix C. To leading order in $\epsilon_L \gg \epsilon_T$ and times $t \gg \tau_u$ one finds

$$\delta^{\mu\mu}\{D_{11}^{\text{eff}}\}(t) = (\pi/2)^{1/2}\, q_0\, \bar{u}\, l_0 \,\{1 - (1 + 4t/\tau_{D_T})^{-(d-1)/2}\} + \cdots, \tag{4.19}$$

$$\delta^{\mu\mu}\{D_{11}^{\text{ens}}\}(t) = (\pi/2)^{1/2}\, q_0\, \bar{u}\, l_0 + \cdots. \tag{4.20}$$

The dots indicate subleading corrections: in both quantities, exponential corrections decay on the τ_u-scale of the form $\sim \exp(-(t/\tau_u)^2/2\,(1 + 2t/\tau_{D_L}))$ which are irrelevant in the regime $t \gg \tau_u$. In the regime $t \gg \tau_{D_T} \gg \tau_{D_L}$ one has corrections of $O(\epsilon_L)$ and $O(\epsilon_T)$ which are subleading for $\epsilon_T \ll \epsilon_L \ll 1$. For times $t \ll \tau_{D_L}$ and times $t \ll \tau_{D_T}$ for the effective dispersion coefficient there are also corrections of the form $\sim \epsilon^n (t/\tau_{D_L})^m$ and $\sim \epsilon^n (t/\tau_{D_T})^m$ with exponents $m, n > 1$ which again are subleading.

Note that the time scale which determines the cross-over from the pre-asymptotic to the final asymptotic behaviour of the effective dispersion coefficient $D^{\text{eff}}(t)$ is indeed set by the *transversal* time scale τ_{D_T}, whereas the longitudinal pore-scale dispersion coefficient D_L only appears in subleading corrections to the given results. This confirms the interpretation put forward in the previous section. The *transversal* microscopic dispersion generates the physical mixing process which ensures that the macroscale dispersion due to advective fluctuations becomes a true physically realized effect also in a single realization of the medium.

Finally, let us mention that the results can also be generalized to the case where the disorder correlations are anisotropic. In a situation with different correlation lengths in different spatial directions, the disorder correlation function (4.5) more generally reads

$$C^{\mu\mu}(\boldsymbol{x}) = \exp\left(-\sum_i x_i^2/2l_i^2 \right), \tag{4.21}$$

where l_i is the correlation length in direction $i = 1 \ldots d$, while x_i denotes the corresponding component of the position vector $\boldsymbol{x}$. In a d-dimensional system, in general, there are now d dispersive time scales which replace the two scales introduced in equation (4.17). They are given by $\tau_{D_L} \equiv l_1^2 / D_L$ (where l_1 is the correlation length in the mean flow direction), and $\tau_{D_{T_i}} \equiv l_i^2 / D_T$ with $i = 2 \ldots d$. Again, as long as the pore-scale dispersion is small, the methods sketched in Appendix C can be applied to extract the leading behaviour of the longitudinal dispersion coefficient. For times $t \gg \tau_u$, equations (4.19) and (4.20) generalize to

$$\delta^{\mu\mu} D_{11}^{\text{eff}}(t) = (\pi/2)^{1/2}\, q_0\, \bar{u}\, l_1 \left\{ 1 - \prod_{i=2}^{d} \left(1 + 4t/\tau_{D_{T_i}}\right)^{-1/2} \right\} + \cdots, \tag{4.22}$$

$$\delta^{\mu\mu} D_{11}^{\text{ens}}(t) = (\pi/2)^{1/2}\, q_0\, \bar{u}\, l_1 + \cdots. \tag{4.23}$$

The explicit results on the transport properties of a non-homogeneously adsorbing medium derived in the previous sections relied on a special choice for the disorder correlation function. Choosing a Gaussian for $C^{\mu\mu}(\boldsymbol{x})$, we have been able to evaluate most of the integrals generated by the perturbation expansion explicitly. In general, however, one expects that the basic features should not depend on this special choice for the correlation function. Also, numerical simulations, e.g. by Burr *et al.* (1994), indicate that the detailed structure of the heterogeneities are relevant only on very short time scales. It can be demonstrated that the leading behaviour of the dispersion coefficients in the various time regimes indeed does not depend on the detailed shape of the disorder correlation function, but only on some simple normalization properties, cf. Attinger (1997).

5. Spatially heterogeneous retardation factor: results for extended initial distributions

The results presented in the previous section can be generalized easily to the more realistic case of an initial concentration distribution of finite extent. For a d-dimensional situation, it is convenient to choose a Gauss-shaped initial distribution for the rescaled transport equation (3.7),

$$\rho(\boldsymbol{x}) = \frac{(2\,\pi)^{-d/2}}{\prod_{i=1}^{d} L_i} \exp\left(-\sum_i x_i^2 / 2\, L_i^2 \right), \tag{5.1}$$

where L_i denotes the initial width of the tracer concentration in direction i ($i = 1 \ldots d$), and x_i the corresponding component of the position vector $\boldsymbol{x}$ in this direction. Note that in the limit of vanishing initial widths $L_i \to 0$ the finite source reduces to the point-source discussed before. To illustrate the basic results, we investigate two different situations. We discuss the case of an isotropically extended distribution, and the results for the extremely anisotropic case of a line-shaped tracer injection.

5.1. *Isotropically extended initial distribution*

The initial distribution $\rho(\boldsymbol{x})$ given by (5.1) becomes isotropic if the widths L_i are the same in all directions, i.e. $L_1 = \cdots = L_d \equiv L$. With this initial concentration, the k'-

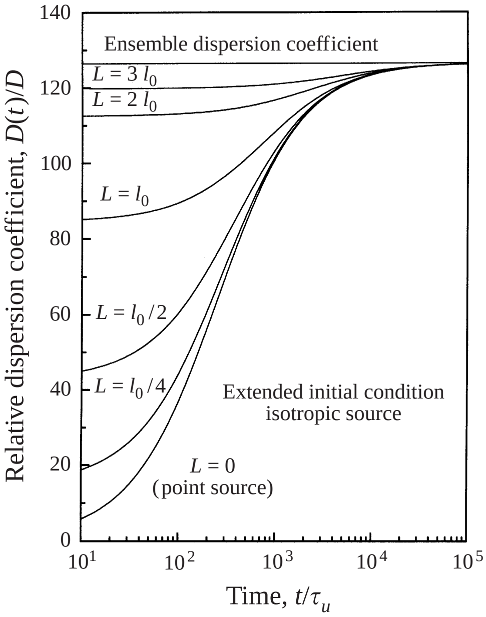

FIGURE 2. Effective and ensemble dispersion coefficients in $d = 3$ as functions of time for times larger than τ'_u in the case of an isotropic initial condition of width L (with $\epsilon = \tau_u/\tau_D = 10^{-3}$ and $q_0 = 10^{-1}$).

integrations in the perturbation theory integrals (A 9) to (A 11) again can be performed explicitly. The resulting expressions are given in Appendix D, equations (D 1) to (D 3). The remaining integrations are very similar to those found for the case of a point-like injection, they yield expressions analogous to those given in (C 1) to (C 3). As the explicit results show, the temporal behaviour of the transport coefficients in this case is governed by four instead of two time scales. In addition to the two scales $\tau_u = l_0/\bar{u}$ and $\tau_D = l_0^2/D$ relevant in the case of a point-like injection, one encounters two new scales given by

$$\tau'_u \equiv \tau_u \left(1 + 2\frac{L^2}{l_0^2}\right)^{1/2} \quad \text{and} \quad \tau'_D \equiv \tau_D \left(1 + 2\frac{L^2}{l_0^2}\right). \tag{5.2}$$

For realistically small values of $\epsilon = D/\bar{u}\,l_0$, the time scales are ordered according to

$$\tau_u \leqslant \tau'_u \ll \tau_D \leqslant \tau'_D. \tag{5.3}$$

The characteristic temporal behaviour found for the ensemble and the effective dispersion coefficients $D_{11}^{\mathrm{ens}}(t)$ and $D_{11}^{\mathrm{eff}}(t)$ are plotted in figure 2 for different sizes of the initial plume. The scales again define different time regimes. Using the arguments of Appendix C, the leading temporal behaviour in these regimes can be derived explicitly for the case of a (realistically) small local dispersion. Not very surprisingly, one finds that the *ensemble* dispersion coefficient $D_{11}^{\mathrm{ens}}(t)$ depends only very weakly on the size of the initial plume. As discussed above, the leading behaviour of $D_{11}^{\mathrm{ens}}(t)$ in the case of a point-like injection is due to the centre-of-mass fluctuations of the evolving plume from sample to sample. The ensemble-averaged concentration distribution includes all these fluctuations and, owing to the translation invariance of the statistical ensemble, no longer depends on the position of the initial injection. As a consequence, any normalized superposition of such solutions again yield the same distribution as before. The solution for the case of an extended initial distribution is such a superposition of point-source solutions, and is therefore independent of the width of the initial source. From this argument one might conclude that the ensemble dispersion coefficient also should show no dependence at all on the finite initial width of the plume – a result which is indeed true e.g. for the case of the dispersion contributions due to fluctuation of the flow field investigated in Dentz (1997) and Dentz *et al.* (1998). For the problem under consideration here, the situation is slightly more subtle since the ensemble dispersion coefficient $D_{11}^{\mathrm{ens}}(t)$ is not derived from the ensemble-averaged concentration, but from the average over the normalized density defined by equation (2.5). The normalizing denominator also contributes to the ensemble dispersion coefficient, but only in an irrelevant way. In figure 2, therefore, there is only one single curve for the ensemble quantity, independent of the width L of the initial distribution. As our explicit results show, it yields corrections of the order of the (small) local dispersion coefficient which are completely negligible compared to the leading behaviour which is determined by (D 1).

In contrast to this result for the ensemble quantity, the transient temporal behaviour of the physically more relevant *effective* quantity $D_{11}^{\mathrm{eff}}(t)$ depends strongly on the initial plume size. One has to distinguish between the various time regimes set by the time scales given above. As before, the behaviour in the short-time regime $t \ll \tau_u$ is of little interest since the cloud has explored only a region in space smaller than the disorder correlation length. For larger times, one now has three different regimes.

First intermediate time regime: $\tau_u \ll t \ll \tau_u'$

The effective dispersion coefficient $D_{11}^{\mathrm{eff}}(t)$ increases quickly, reaching a plateau value smaller than the final asymptotic limit. The difference between this plateau value and infinite time coefficient, however, decreases with increasing initial width of the plume. In the limiting case of an extremely large initial extent of the plume (i.e. $l_0 \ll L \to \infty$) the plateau value approaches the infinite time value, in this case the effective dispersion coefficient has already converged to the ensemble behaviour given by $D_{11}^{\mathrm{ens}}(t)$ within the given time-regime.

Second intermediate time regime: $\tau_u' \ll t \ll \tau_D'$

In this regime, the effective dispersion coefficient $D_{11}^{\mathrm{eff}}(t)$ remains almost constant at the plateau value. There is a weak linear time dependence comparable to the linear regime found in the case of a point source. Note that the time scale τ_D which was the most relevant one in the case of a point-like injection lies within the given regime. It has, however, completely lost its leading role. It is of relevance only for small subleading modifications which are of the order of the (negligibly small) local dispersion coefficient. If one neglects the local dispersion coefficient from the beginning, starting from a model with $D \equiv 0$, the time scales τ_D and τ_D' become infinite. In this case the intermediate time regime extends to infinite times and also determines the long-time asymptotics of the quantities. In this case, the asymptotic limit of the effective dispersion coefficient is given by the aforementioned plateau value which depends on the size of the initial plume and remains smaller than the corresponding ensemble value, a fact discussed already by Dagan (1991) in the context of his Lagrangian analysis of the random flow problem without local dispersion. For finite local dispersion coefficients, however, the system enters a new long-time regime for times larger than the time scale τ_D' which now is finite. (In passing, let us note that a recent paper by Fiori (1998) which tries to extend Dagan's analysis of the infinite-time asymptotics to include the effects of a finite local dispersion actually treats the dispersion corrections to the plateau value of the second intermediate time-regime. Owing to technical restrictions of his method, the infinite-time limit misses the final crossover to the true long-time regime, see Dentz & Kinzelbach (1998).)

Long-time regime: $t \gg \tau'_D$

In the final long-time regime, the effective dispersion coefficient $D^{\mathrm{eff}}_{11}(t)$ becomes almost independent of the initial plume size. Hence, we end up with the same preasymptotic power-law behaviour found in the case of the point-like injection for $t \gg \tau_D$, cf. § 4. Note, however, that this statement has a somewhat restricted meaning: the time scale τ'_D which defines this regime increases with increasing extent of the initial distribution. So in the limit of an extremely large initial source (i.e. $L \to \infty$) this regime becomes unreachable and $D^{\mathrm{eff}}_{11}(t)$ shows a temporal behaviour identical to $D^{\mathrm{ens}}_{11}(t)$.

Using the methods discussed in Appendix C the results follow explicitly from the perturbation theory expressions. In the (realistic) case of a small $\epsilon = D/\bar{u}\, l_0 \ll 1$ and times $t \gg \tau'_u$, the leading behaviour of the ensemble dispersion coefficient is given by $\delta^{\mu\mu}\{D^{\mathrm{ens}}_{11}\}(t) = (\pi/2)^{1/2}\, q_0\, \bar{u}\, l_0 + \cdots$, a result identical to that in the case of a point-like injection. The result for the corresponding effective quantity in the same time regime reads

$$\delta^{\mu\mu}\{D^{\mathrm{eff}}_{11}\}(t) = (\pi/2)^{1/2}\, q_0\, \bar{u}\, l_0 \left\{ 1 - \frac{1}{(1 + 2L^2/l_0^2)^{(d-1)/2}\,(1 + 4t/\tau'_D)^{(d-1)/2}} \right\} + \cdots . \tag{5.4}$$

The expression reduces to the one found for the point source in the limiting case $L \to 0$, cf. equation (4.19). As mentioned above, it reaches an intermediate plateau value for times $\tau'_u \ll t \ll \tau'_D$. From the previous equation, this plateau value can be read off as $(\pi/2)^{1/2}\, q_0\, \bar{u}\, l_0\, \{1 - (1 + 2L^2/l_0^2)^{-(d-1)/2}\}$. It vanishes in the limit of a point-like tracer injection $L \to 0$, and approaches $\delta^{\mu\mu}\{D^{\mathrm{ens}}\}(\infty) = (\pi/2)^{1/2}\, q_0\, \bar{u}\, l_0$ in the case of an infinitely extended initial distribution $L \to \infty$.

5.2. *Anisotropical initial condition: line source*

The distribution of the source in realistic field situations is usually found to be anisotropic, see e.g. Burr *et al.* (1994). Typically, its width is small compared to the soil correlation length in the horizontal direction, but extends over quite some correlation lengths in the vertical direction. From a slightly simplified point of view, it is given by a vertically aligned, line-shaped source distribution. Starting from the general distribution (5.1) (with $d = 3$), this corresponds to the anisotropic limit $L_1 = L_2 \to 0$, while keeping the length in the vertical direction, $L_3 > 0$, fixed. The distribution reduces to

$$\rho(\boldsymbol{x}) = \delta(x_1)\, \delta(x_2)\, (2\,\pi)^{-1/2}\, \exp(-x_3^2/2\,L_3^2). \tag{5.5}$$

In this case the two advective time scales τ_u and τ'_u introduced above coincide, so the temporal behaviour of the transport properties is characterized by the remaining three time scales, τ_u, τ_D, and $\tau'_D = \tau_D(1 + 2L_3^2/l_0^2)$. The corresponding explicit perturbation theory results are plotted in figure 3 for the time regime $t > \tau_u$. For the reasons discussed in the previous section, the ensemble coefficient is almost independent of the initial length L. So figure 3, too, shows only one single curve for D^{ens}. The corresponding effective dispersion coefficient, however, does depend on L. Its properties follow from the explicit expressions given in Appendix D. For the leading

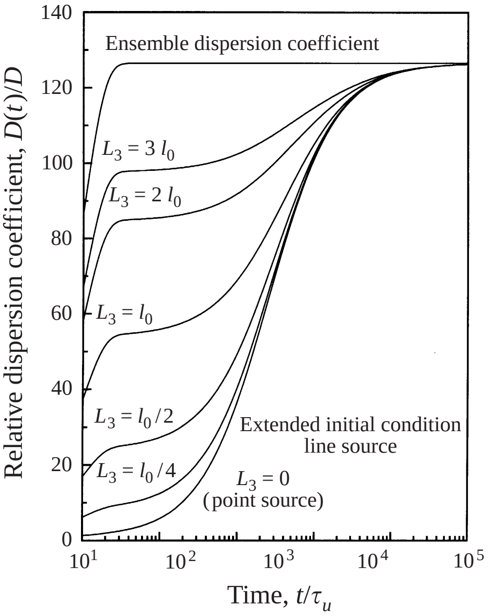

FIGURE 3. Effective and ensemble dispersion coefficients in $d = 3$ as functions of time for times larger than $\tau_u = \tau_u'$ in the case of a line-shaped initial condition of length L_3, aligned perpendicular to the mean flow direction (with $\epsilon = \tau_u/\tau_D = 10^{-3}$ and $q_0 = 10^{-1}$).

behaviour for $t \gg \tau_u$ one finds

$$\delta^{\mu\mu}\{D_{11}^{\mathrm{eff}}\}(t) = (\pi/2)^{1/2}\, q_0\, \overline{u}\, l_0 \left\{1 - \frac{1}{(1+2L_3^2/l_0^2)^{1/2}(1+4t/\tau_D)^{1/2}(1+4t/\tau_D')^{1/2}}\right\}. \tag{5.6}$$

Again the most characteristic difference to the case of a point source discussed in §4 is the plateau value of $D_{11}^{\mathrm{eff}}(t)$ found also in the isotropic case of the previous section. For the line source, this plateau dominates the time regime $\tau_u \ll t \ll \tau_D$. The corresponding plateau value is given by $(\pi/2)^{1/2}\, q_0 \overline{u}\, l_0\, \{1 - (1 + 2L_3^2/l_0^2)^{-1/2}\}$. It is remarkedly smaller than the value found in the isotropic situation, so for the given (practically more relevant) anisotropic initial condition, the difference between effective and ensemble quantities at finite times is much more pronounced than in the isotropic case. For times $t \gg \tau_D$ again the asymptotic long-time limit is approached algebraically. In principle, in cases where the two dispersive scales τ_D and τ_D' are well separated (i.e. for $L_3 \gg l_0$) one may distinguish two different regimes $\tau_D \ll t \ll \tau_D'$ and $\tau_D' \ll t$ with leading powers $t^{-1/2}$ and t^{-1}, respectively, in the three-dimensional situation. Note, however, that in this case also the plateau value is already close to the final asymptotic dispersion coefficient, so these two regimes are hardly visible.

6. Summary

A porous medium with a retardation coefficient varying stochastically in space was taken as a model for investigating the temporal behaviour of effective transport properties. For a point-like injection of solute at time $t = 0$ the explicit perturbative solutions for the time evolution of the first and second moments of the solute cloud were derived up to second order. From these, two fundamentally different quantities were defined: the effective dispersion coefficient D^{eff}, representing the physically realized (and observable) dispersion in a typical realization of the aquifer and the mathematically simpler ensemble dispersion coefficient D^{ens}, characterizing the fluctuations from realization to realization within the ensemble. The temporal behaviour of the two quantities is remarkably different for the point source. The ensemble quantity $D^{\mathrm{ens}}(t)$ reaches its final asymptotic value on time scale τ_u with a fast exponential approach to this asymptotic value. The effective quantity $D^{\mathrm{eff}}(t)$, which gives a more faithful representation of the real mixing behaviour characteristic of a given typical aquifer realization, reaches its long-time asymptotic value only on the much larger time scale $\tau_D \gg \tau_u$. The approach is slow and for times $t \gg \tau_D$ it follows an inverse power law, $\sim (t/\tau_D)^{-(d-1)/2}$. In a real aquifer situation where the system is finite, it may well happen that this limit is not reached within the given system boundaries. For times $t \ll \tau_D$, the ensemble dispersion coefficient $D^{\mathrm{ens}}(t)$ usually discussed in the literature, considerably overestimates the true pre-asymptotic dispersion found in one aquifer realization. This has also been observed in numerical simulations on single realizations of a stochastic medium.

The method presented here allows the systematic calculation of both effective and ensemble quantities. By choosing a Gaussian disorder correlation function we have been able to evaluate the perturbation expressions explicitly without any further approximations. In the practically most relevant case $\epsilon = D/\bar{u}l_0 \ll 1$, the technical effort can be reduced considerably by further approximations. In this case it is also possible to derive the leading time behaviour of the quantities of interest for more general situations such as anisotropic local dispersion coefficients, anisotropic heterogeneity, and an extended source. The generalization of the results to a source of finite size shows that with increasing size the differences between $D^{\mathrm{eff}}(t)$ and $D^{\mathrm{ens}}(t)$ vanish even at small times on the order of τ_u. This is intuitively clear, as an extended source samples the aquifer faster and is therefore equivalent to an ensemble of point sources. Consequently, the transport parameters for a typical single realization should, with growing size of the source, approach the ensemble quantities. This approach is the faster the larger the source is compared to the correlation length of the medium. The differences will become neglibible if in at least one coordinate direction the source is larger than 10 times the correlation length. In real aquifers the extent of a source in the vertical direction is most likely to be on the order of or larger than the corresponding correlation length, while in the horizontal directions a tracer or pollutant injection can usually be considered point-like. Yet, in aquifers containing multiple scales the point source approximation even in the vertical direction may still be of considerable interest.

The method can be extended straightforwardly to take into account higher-order corrections of the perturbation theory and to treat models which include other random processes. As the calculations by Dentz (1997) and Dentz *et al.* (1998) show, the conclusions and interpretations discussed here remain qualitatively unchanged in the more general model which allows for fluctuations both in the hydraulic conductivities and the retardation factor.

Dedicated to Heinz Horner on the occasion of his 60th birthday. It is a pleasure to thank Heinz Horner, Dirk Metzger, Insa Neuweiler and Rolf Reichle for many helpful discussions.

Appendix A. Spatial retardation fluctuations: perturbation theory expressions

From equations (3.17) to (3.19) and the perturbation series (3.22), one gets the following expressions for the disorder-induced corrections due to the spatial fluctuations of the retardation factor:

$$\delta^{\mu\mu}\{u_j^{\mathrm{eff}}\}(t) = (-\mathrm{i}\partial_{k_j})\,\partial_t\,\{I_1(\boldsymbol{k},t) - \tfrac{1}{2}\,I_2(\boldsymbol{k},\boldsymbol{k},t)\}\big|_{\boldsymbol{k}=0}, \tag{A 1}$$

$$\delta^{\mu\mu}\{D_{ij}^{\mathrm{eff}}\}(t) = (-\mathrm{i}\partial_{k_i})\,(-\mathrm{i}\partial_{k_j})\,\partial_t\{I_1(\boldsymbol{k},t) - \tfrac{1}{2}\,I_2(\boldsymbol{k},\boldsymbol{k},t)\}\big|_{\boldsymbol{k}=0}, \tag{A 2}$$

$$\delta^{\mu\mu}\{D_{ij}^{\mathrm{ens}}\}(t) = (-\mathrm{i}\partial_{k_i})\,(-\mathrm{i}\partial_{k_j})\,\partial_t\{I_1(\boldsymbol{k},t) - I_2(0,\boldsymbol{k},t)\}\big|_{\boldsymbol{k}=0}, \tag{A 3}$$

with functions $I_1(\boldsymbol{k},t)$ and $I_2(\boldsymbol{k}_1,\boldsymbol{k}_2,t)$ given by

$$\begin{aligned} I_1(\boldsymbol{k},t) \equiv{}& \tilde{g}_0(\boldsymbol{k},t)^{-1}\int_{-\infty}^{+\infty}\mathrm{d}t'\,\mathrm{d}t''\int_{\boldsymbol{k}'}\widetilde{C}^{\mu\mu}(\boldsymbol{k}')\,\tilde{g}_0(\boldsymbol{k},t-t')\\ &\times\partial_{t'}\tilde{g}_0(\boldsymbol{k}-\boldsymbol{k}',t'-t'')\,\partial_{t''}\tilde{g}_0(\boldsymbol{k},t''), \end{aligned} \tag{A 4}$$

$$\begin{aligned} I_2(\boldsymbol{k}_1,\boldsymbol{k}_2,t) \equiv{}& \tilde{g}_0(\boldsymbol{k}_1,t)^{-1}\,\tilde{\rho}(\boldsymbol{k}_1)^{-1}\,\tilde{g}_0(\boldsymbol{k}_2,t)^{-1}\,\tilde{\rho}(\boldsymbol{k}_2)^{-1}\\ &\times\int_{-\infty}^{+\infty}\mathrm{d}t'\,\mathrm{d}t''\int_{\boldsymbol{k}'}\widetilde{C}^{\mu\mu}(\boldsymbol{k}')\,\tilde{g}_0(\boldsymbol{k}_1,t-t')\,\partial_{t'}\tilde{g}_0(\boldsymbol{k}_1-\boldsymbol{k}',t')\\ &\times\tilde{\rho}(\boldsymbol{k}_1-\boldsymbol{k}')\,\tilde{g}_0(\boldsymbol{k}_2,t-t'')\,\partial_{t''}\tilde{g}_0(\boldsymbol{k}_2+\boldsymbol{k}',t'')\,\tilde{\rho}(\boldsymbol{k}_2+\boldsymbol{k}'), \end{aligned} \tag{A 5}$$

where $\widetilde{C}^{\mu\mu}(\boldsymbol{k})$ is the Fourier transform of the disorder correlation function $C^{\mu\mu}(\boldsymbol{x})$ given in (3.4), $\widetilde{C}^{\mu\mu}(\boldsymbol{k}) = \int \mathrm{d}^d x\; C^{\mu\mu}(\boldsymbol{x})\;\exp(\mathrm{i}\boldsymbol{k}\cdot\boldsymbol{x})$. Analogously, $\tilde{\rho}(\boldsymbol{k})$ is the Fourier transform of the initial tracer concentration $c(\boldsymbol{x},t=0) = \rho(\boldsymbol{x})$.

By partial integrations with respect to t' and t'' it is possible to replace the two internal time derivatives in (A 4) and (A 5) by derivatives with respect to the external time variable t. Regrouping the equations for $u_\mu^{\mathrm{eff}}(t)$, $D_{ij}^{\mathrm{eff}}(t)$, and $D_{ij}^{\mathrm{ens}}(t)$ in a way more appropriate for the following calculations, we get

$$\delta^{\mu\mu}\{u_j^{\mathrm{eff}}\}(t) = 2\,\bar{u}\;\partial_t[B_1(0,t) - \tfrac{1}{2}\,B_2(0,t)]\delta_{j1} + \tfrac{1}{2}\;\delta_{j1}\;(-\mathrm{i}\partial_{k_1})\,\partial_t^2\;B_1(\boldsymbol{k},t)\;\big|_{\boldsymbol{k}=0}, \tag{A 6}$$

$$\begin{aligned} \delta^{\mu\mu}\{D_{ij}^{\mathrm{eff}}\}(t) ={}& \bar{u}^2\;[B_1(0,t) - B_2(0,t)]\;\delta_{i1}\,\delta_{j1}\\ &+2\{D_{ij} + \bar{u}\,\delta_{i1}\,(-\mathrm{i}\partial_{k_j})\}\;\partial_t[B_1(\boldsymbol{k},t) - \tfrac{1}{2}\,B_2(\boldsymbol{k},t)]_{\boldsymbol{k}=0}\\ &+\tfrac{1}{2}(-\mathrm{i}\partial_{k_i})\,(-\mathrm{i}\partial_{k_j})\,\partial_t^2\;B_1(\boldsymbol{k},t)\big|_{\boldsymbol{k}=0}, \end{aligned} \tag{A 7}$$

$$\begin{aligned} \delta^{\mu\mu}\{D_{ij}^{\mathrm{ens}}\}(t) ={}& \bar{u}^2\;B_1(0,t)\;\delta_{i1}\,\delta_{j1}\\ &+2\{D_{ij} + \bar{u}\,\delta_{i1}\,(-\mathrm{i}\partial_{k_j})\}\;\partial_t\;[B_1(\boldsymbol{k},t) - \tfrac{1}{2}\,B_3(\boldsymbol{k},t)]_{\boldsymbol{k}=0}\\ &+\tfrac{1}{2}\;((-\mathrm{i}\partial_{k_i})\,(-\mathrm{i}\partial_{k_j})\,\partial_t^2\;B_1(\boldsymbol{k},t)\big|_{\boldsymbol{k}=0}, \end{aligned} \tag{A 8}$$

with functions $B_1(\boldsymbol{k},t)$, $B_2(\boldsymbol{k},t)$, and $B_3(\boldsymbol{k},t)$ given by

$$B_1(\boldsymbol{k},t) = q_0\int_0^t\mathrm{d}t'\int_{\boldsymbol{k}'}\widetilde{C}^{\mu\mu}(\boldsymbol{k}')\;\exp\{-(\mathrm{i}\bar{u}\;\boldsymbol{n}(\boldsymbol{k})\cdot\boldsymbol{k}' + \boldsymbol{k}'\cdot\boldsymbol{D}\cdot\boldsymbol{k}')t'\}, \tag{A 9}$$

$$\begin{aligned} B_2(\boldsymbol{k},t) ={}& q_0\;\tilde{\rho}(\boldsymbol{k})^{-2}\int_0^t\mathrm{d}t'\int_{\boldsymbol{k}'}\widetilde{C}^{\mu\mu}(\boldsymbol{k}')\,\tilde{\rho}(\boldsymbol{k}-\boldsymbol{k}')\;\tilde{\rho}(\boldsymbol{k}+\boldsymbol{k}')\\ &\times\exp\{-\mathrm{i}\bar{u}\;\boldsymbol{n}(\boldsymbol{k})\cdot\boldsymbol{k}'\,(t-t') - \boldsymbol{k}'\cdot\boldsymbol{D}\cdot\boldsymbol{k}'\;(t+t')\}, \end{aligned} \tag{A 10}$$

$$B_3(\boldsymbol{k},t) = q_0\,\widetilde{\rho}(\boldsymbol{k})^{-1}\int_0^t \mathrm{d}t' \int_{\boldsymbol{k}'} \widetilde{C}^{\mu\mu}(\boldsymbol{k}')\,\widetilde{\rho}(\boldsymbol{k}-\boldsymbol{k}')\,\widetilde{\rho}(\boldsymbol{k}').$$
$$\times \exp\{-\mathrm{i}\,\bar{u}\,\boldsymbol{k}'\cdot(\boldsymbol{e}_1\,t - \boldsymbol{n}(\boldsymbol{k})\,t') - \boldsymbol{k}'\cdot\boldsymbol{\mathsf{D}}\cdot\boldsymbol{k}'\,(t+t')\}, \tag{A 11}$$

where $\boldsymbol{e}_1$ is the unit vector in the direction of the advective flow field $\bar{\boldsymbol{u}}$ (i.e. in the 1-direction), and where we introduced the auxiliary vector

$$\boldsymbol{n}(\boldsymbol{k}) \equiv \boldsymbol{e}_1 + \frac{2D}{\bar{u}}\mathrm{i}\boldsymbol{k}. \tag{A 12}$$

Appendix B. Point-like injection: explicit results

In the case of a point-like injection the initial concentration $\rho(\boldsymbol{x})$ is $\rho(\boldsymbol{x}) = \delta^d(\boldsymbol{x})$ and its Fourier transform $\rho(\boldsymbol{k}) = 1$. For the Gaussian disorder correlation function given in (4.6), the $\boldsymbol{k}'$-integrations in (A 9) to (A 11) can be performed explicitly. In the case of an isotropic local dispersion tensor, i.e. for $D_L = D_T \equiv D$ in equation (3.9), one ends up with

$$B_1(\boldsymbol{k},t) = q_0 \int_0^t \mathrm{d}t'\,(1+2t'/\tau_D)^{-d/2}\,\exp(\frac{-(\boldsymbol{n}(\boldsymbol{k})\,t'/\tau_u)^2}{2\,(1+2t'/\tau_D)}), \tag{B 1}$$

$$B_2(\boldsymbol{k},t) = q_0\,(1+4t/\tau_D)^{-d/2}\int_0^t \mathrm{d}t'\,(1-\frac{2t'/\tau_D}{1+4t/\tau_D})^{-d/2}$$
$$\times \exp\left(\frac{-(\boldsymbol{n}(\boldsymbol{k})\,t'/\tau_u)^2}{2\,(1+4t/\tau_D)}\left(1-\frac{2t'/\tau_D}{1+4t/\tau_D}\right)^{-1}\right), \tag{B 2}$$

$$B_3(\boldsymbol{k},t) = q_0\,\left(1+4t/\tau_D\right)^{-d/2}\int_0^t \mathrm{d}t'\left(1-\frac{2t'/\tau_D}{1+4t/\tau_D}\right)^{-d/2}$$
$$\times \exp\left(\frac{-(\boldsymbol{n}(\boldsymbol{k})\,t'/\tau_u - 2\mathrm{i}\,l_0\,\boldsymbol{k}\,t/\tau_D)^2}{2\,(1+4t/\tau_D)}\left(1-\frac{2t'/\tau_D}{1+4t/\tau_D}\right)^{-1}\right), \tag{B 3}$$

with time scales $\tau_u = l_0/\bar{u}$ and $\tau_D = l_0^2/D$.

For $d = 1$ and $d = 3$, the remaining integrations can be performed explicitly, using extensively the formulae given in Gradshteyn & Ryzhik (1980) and Abramowitz & Stegun (1972). We find the following expressions:

$$B_1(\boldsymbol{k},t,d=3) = \frac{\pi^{1/2}}{2}\frac{\tau_D}{v(\boldsymbol{k})}\,\{\mathrm{erf}(v(\boldsymbol{k})\,(t/\tau_D)\;T_2(t)^{-1/2})$$
$$-\exp(v(\boldsymbol{k})^2)[\mathrm{erf}(v(\boldsymbol{k})) - \mathrm{erf}(v(\boldsymbol{k})\;T_1(t)\;T_2(t)^{-1/2})]\},$$

$$B_1(\boldsymbol{k},t,d=1) = \frac{\pi^{1/2}}{2}\frac{\tau_D}{v(\boldsymbol{k})}\,\{\mathrm{erf}(v(\boldsymbol{k})\,(t/\tau_D)\;T_2(t)^{-1/2})$$
$$+\exp(v(\boldsymbol{k})^2)[\mathrm{erf}(v(\boldsymbol{k})) - \mathrm{erf}(v(\boldsymbol{k})\;T_1(t)\;T_2(t)^{-1/2})]\},$$

$$B_2(\boldsymbol{k},t,d=3) = \frac{\pi^{1/2}}{2}\frac{\tau_D}{v(\boldsymbol{k})}\;T_4(t)^{-1}\{\mathrm{erf}(v(\boldsymbol{k})\,(t/\tau_D)\;T_2(t)^{-1/2})$$
$$-\exp(v(\boldsymbol{k})^2\;T_4(t))[\mathrm{erf}(v(\boldsymbol{k})\;T_4(t)^{1/2}) - \mathrm{erf}(v(\boldsymbol{k})\;T_3(t)\;T_2(t)^{-1/2})]\},$$

$$B_2(\boldsymbol{k},t,d=1) = \frac{\pi^{1/2}}{2}\frac{\tau_D}{v(\boldsymbol{k})}\{\mathrm{erf}(v(\boldsymbol{k})\,(t/\tau_D)\;T_2(t)^{-1/2})$$
$$+\exp(v(\boldsymbol{k})^2\;T_4(t))[\mathrm{erf}(v(\boldsymbol{k})\;T_4(t)^{1/2}) - \mathrm{erf}(v(\boldsymbol{k})\;T_3(t)\;T_2(t)^{-1/2})]\},$$

$$\begin{aligned}
B_3(\boldsymbol{k},t,d=3) = {} & \frac{\pi^{1/2}}{2}\frac{\tau_D}{\widetilde{v}(\boldsymbol{k})}\ \exp(\tfrac{1}{2}\ \boldsymbol{N}(\boldsymbol{k})\cdot\widetilde{\boldsymbol{N}}(\boldsymbol{k})) \\
& \times\{\exp(\tfrac{1}{2}v(\boldsymbol{k})\widetilde{v}(\boldsymbol{k}))\,\mathrm{erf}(\tfrac{1}{2}v(\boldsymbol{k})\ T_4(t)^{1/2}+\tfrac{1}{2}\widetilde{v}(\boldsymbol{k})\ T_4(t)^{-1/2}) \\
& -\exp(-\tfrac{1}{2}v(\boldsymbol{k})\widetilde{v}(\boldsymbol{k}))\,\mathrm{erf}(\tfrac{1}{2}v(\boldsymbol{k})\ T_4(t)^{1/2}-\tfrac{1}{2}\widetilde{v}(\boldsymbol{k})\ T_4(t)^{-1/2}) \\
& -\exp(\tfrac{1}{2}v(\boldsymbol{k})\widetilde{v}(\boldsymbol{k}))\,\mathrm{erf}(\tfrac{1}{2}v(\boldsymbol{k})\ T_2(t)^{1/2}+\tfrac{1}{2}\widetilde{v}(\boldsymbol{k})\ T_2(t)^{-1/2}) \\
& +\exp(-\tfrac{1}{2}v(\boldsymbol{k})\widetilde{v}(\boldsymbol{k}))\,\mathrm{erf}(\tfrac{1}{2}v(\boldsymbol{k})\ T_2(t)^{1/2}-\tfrac{1}{2}\widetilde{v}(\boldsymbol{k})\ T_2(t)^{-1/2})\}, \\
B_3(\boldsymbol{k},t,d=1) = {} & \frac{\pi^{1/2}}{2}\frac{\tau_D}{v(\boldsymbol{k})}\ \{\mathrm{erf}(2^{-1/2}\,(t/\tau_u)\ T_2(t)^{-1/2}) \\
& +\mathrm{erf}(2^{1/2}\,(t/\tau_u)\ T_4(t)^{-1/2}\,\epsilon\, l_0\,\mathrm{i}\boldsymbol{k}) \\
& +\exp(\tfrac{1}{2}v(\boldsymbol{k})\widetilde{v}(\boldsymbol{k}))\,\mathrm{erf}(\tfrac{1}{2}v(\boldsymbol{k})\ T_4(t)^{1/2}+\tfrac{1}{2}\widetilde{v}(\boldsymbol{k})\ T_4(t)^{-1/2}) \\
& -\exp(\tfrac{1}{2}v(\boldsymbol{k})\widetilde{v}(\boldsymbol{k}))\,\mathrm{erf}(\tfrac{1}{2}v(\boldsymbol{k})\ T_2(t)^{1/2}+\tfrac{1}{2}\widetilde{v}(\boldsymbol{k})\ T_2(t)^{-1/2})\},
\end{aligned}$$

with

$$\begin{aligned}
&\boldsymbol{N}(\boldsymbol{k}) \equiv \boldsymbol{n}(\boldsymbol{k})\,(2\,\epsilon^2)^{-1/2} = (\boldsymbol{e}_1+2\mathrm{i}\boldsymbol{k}\,l_0\,\epsilon)\,(2\,\epsilon^2)^{-1/2}, \\
&\widetilde{\boldsymbol{N}}(\boldsymbol{k}) \equiv (\boldsymbol{n}(\boldsymbol{k})+(2\,t/\tau_D)\,(\boldsymbol{n}(\boldsymbol{k})+\boldsymbol{e}_1))\,(2\,\epsilon^2)^{-1/2} = \boldsymbol{N}(\boldsymbol{k})+(4\,t/\tau_D)\,\boldsymbol{N}(\boldsymbol{k}/2), \\
&v(\boldsymbol{k}) \equiv (\boldsymbol{N}^2(\boldsymbol{k}))^{1/2}, \quad \widetilde{v}(\boldsymbol{k}) \equiv (\widetilde{\boldsymbol{N}}^2(\boldsymbol{k}))^{1/2}, \\
&T_m(t) \equiv 1+m\,t/\tau_D \quad \text{with} \quad m=1,2,3,4.
\end{aligned}$$

Inserting these lengthy expressions into (A 6) to (A 8) eventually yields explicit results for $u^{\mathrm{eff}}(t)$, $D^{\mathrm{eff}}(t)$, and $D^{\mathrm{ens}}(t)$. To evaluate the various derivatives with respect to $\boldsymbol{k}$ given in these formulae is an elementary but tedious task. One ends up with a large number of different additive contributions. It is useful to perform this last step using a computer-algebra program like MAPLE or MATHEMATICA.

Appendix C. Point-like injection: results for a small pore-scale dispersion

In the case $\epsilon_T \ll \epsilon_L \ll 1$, it is possible to extract the leading temporal behaviour of all integral expressions involved for arbitrary space dimensions d. We investigate the regime $t \gg \tau_u$. In B_1, the main contribution to the integral comes from the region of integration where the integration variable t' is small. For increasing $t' > \tau_u$, the integrand vanishes exponentially fast. If we rewrite the integration according to $\int_0^t = \int_0^\infty - \int_t^\infty$, the time-dependent part $\int_t^\infty$ also vanishes exponentially fast for $t \gg \tau_u$, leading to a negligibly small correction in the time regime under consideration. The time-independent part $\int_0^\infty$ can be evaluated if one expands with respect to D_L and D_T, i.e. with respect to the dimensionless quantities ϵ_L and ϵ_T. To leading order, for small values of ϵ_L and ϵ_T one ends up with

$$B_1(\boldsymbol{k},t) = q_0\frac{\pi^{1/2}}{2}\frac{\tau_u}{(\boldsymbol{n}(\boldsymbol{k})^2)^{1/2}}\{1+\cdots\} \tag{C 1}$$

where the dots denote corrections of $O(\epsilon_L)$ and $O(\epsilon_T)$. In B_2 and B_3 we expand the integrands with respect to $2(t'/\tau_{D_L})/(1+4t/\tau_{D_L})$ and $2(t'/\tau_{D_T})/(1+4t/\tau_{D_T})$ which is smaller than 1 for all t'. In the corresponding leading expression we again replace the upper integration boundary by ∞. A more careful investigation of the neglected correction terms reveals that the approximation loses only negligibly small exponential corrections whereas the expansion performed first generates corrections which in the time regime $t \ll \tau_{D_L} \ll \tau_{D_T}$ are of higher order in ϵ_L or ϵ_T, and which are of higher orders in $(t/\tau_{D_L})^{-1}$ or $(t/\tau_{D_T})^{-1}$ for $t \gg \tau_{D_T} \gg \tau_{D_L}$. The leading behaviour for $\epsilon_T \ll \epsilon_L \ll 1$ is given by

$$B_2(\boldsymbol{k},t) = q_0(\pi/2)^{1/2}\,\frac{\tau_u}{(\boldsymbol{n}(\boldsymbol{k})^2)^{1/2}}\,(1+4t/\tau_{D_T})^{-(d-1)/2}\,\{1+\cdots\}, \tag{C 2}$$

$$\begin{aligned} B_3(\boldsymbol{k},t) = {} & q_0(\pi/2)^{1/2}\,\frac{\tau_u}{(\boldsymbol{n}(\boldsymbol{k})^2)^{1/2}}\,(1+4t/\tau_{D_T})^{-(d-1)/2}\,\mathrm{erfc}\Big(-\mathrm{i}\boldsymbol{k}\cdot\boldsymbol{e}_1\,\frac{2^{1/2}\,l_0\,t/\tau_{D_L}}{(1+4t/\tau_{D_L})^{1/2}}\Big) \\ & \times \exp\Big\{2\,\frac{(l_0\,t/\tau_{D_L})^2}{1+4t/\tau_{D_L}}\,(\boldsymbol{k}^2-(\boldsymbol{k}\cdot\boldsymbol{e}_1)^2)\Big\}\{1+\cdots\}. \end{aligned} \tag{C 3}$$

With these results, the expressions for D_{11}^{eff} and D_{11}^{ens}, equations (A 7) and (A 8), reduce to those given in (4.19) and (4.20) for $t \gg \tau_u$ and $\epsilon_T = D_T/\bar{u}\,l_0 \ll \epsilon_L = D_L/\bar{u}\,l_0 \ll 1$.

Appendix D. Finite source: explicit results

In the case of a finite source $\rho(\boldsymbol{x})$ given by a Gaussian it is again possible to perform the $\boldsymbol{k}'$ integration in (A 9) to (A 11) explicitly. For a Gaussian disorder correlation function given by (4.6) and an isotropic local dispersion tensor, i.e. for $D_L = D_T \equiv D$ in equation (3.9), one ends up with

$$B_1(\boldsymbol{k},t) = q_0 \int_0^t \mathrm{d}t'\,\left(1+2t'/\tau_D\right)^{-d/2}\,\exp\left(\frac{-(\boldsymbol{n}(\boldsymbol{k})\;t'/\tau_u)^2}{2\,(1+2t'/\tau_D)}\right), \tag{D 1}$$

$$\begin{aligned} B_2(\boldsymbol{k},t) = {} & q_0\,\left(\frac{l_0}{L^*}\right)^d\,(1+4t/\tau'_D)^{-d/2}\int_0^t \mathrm{d}t'\,\left(1-\frac{2t'/\tau'_D}{1+4t/\tau'_D}\right)^{-d/2} \\ & \times\,\exp\left(\frac{-(\boldsymbol{n}(\boldsymbol{k})\,t'/\tau'_u)^2}{2\,(1+4t/\tau'_D)}\,\left(1-\frac{2t'/\tau'_D}{1+4t/\tau'_D}\right)^{-1}\right), \end{aligned} \tag{D 2}$$

$$\begin{aligned} B_3(\boldsymbol{k},t) = {} & q_0\,\left(\frac{l_0}{L^*}\right)^d\,(1+4t/\tau'_D)^{-d/2}\int_0^t \mathrm{d}t'\,\left(1-\frac{2t'/\tau'_D}{1+4t/\tau'_D}\right)^{-d/2} \\ & \times\exp\left(\frac{-(\boldsymbol{n}(\boldsymbol{k})\,t'/\tau'_u-2\mathrm{i}\,l_0\,\boldsymbol{k}\,t/\tau'_D)^2}{2\,(1+4t/\tau'_D)}\,\left(1-\frac{2t'/\tau'_D}{1+4t/\tau'_D}\right)^{-1}\right), \end{aligned} \tag{D 3}$$

where L^* is defined by $L^* \equiv l_0\,(1+2L^2/l_0^2)^{1/2}$. The integral expressions depend now on the old time scales $\tau_u = l_0/\bar{u}$ and $\tau_D = l_0^2/D$, and on the new scales $\tau'_u \equiv \tau_u\,(1+2L^2/l_0^2)^{1/2}$ and $\tau'_D \equiv \tau_D\,(1+2L^2/l_0^2)$. The integral (D 1) which gives the ensemble dispersion coefficient $D_{11}^{\mathrm{ens}}(t)$ to leading order for times large compared to the advective time scale, $t \gg \tau_u$, is completely independent of the initial condition. The finite source modifies only the integral expressions (D 2) and (D 3) which determine the behaviour of the effective dispersion coefficient $D_{11}^{\mathrm{eff}}(t)$. The integrals (D 2) and (D 3), however, follow from the corresponding expressions (B 2) and (B 3) for the point source by a simple transformation of the time scales involved: τ_u is replaced by τ'_u and τ_D by τ'_D. Additionally, the integrals are multiplied by a factor $(1+2L^2/l_0^2)^{-d/2}$.

The further treatment is straightforward. We use the same approximations as given in Appendix C to end up with the results presented in § 5.

This discussion can be generalized to the case of an anisotropic initial condition with $L_1 \neq L_2 \neq L_3$ in equation (5.1). In the following, we give the explicit results for $B_1(\boldsymbol{k}, t, d = 3)$ and $B_2(\boldsymbol{k}, t, d = 3)$ for this more general case since this allows us also to treat the line source discussed in § 5.2. Starting from the general anisotropic initial condition, one has six instead of four time scales, given by: τ_u, $\tau'_u \equiv \tau_u(1+2L_1^2/l_0^2)^{1/2}$, τ_D, $\tau'_{D1} \equiv \tau_D\,(1 + 2L_1^2/l_0^2)$, $\tau'_{D2} \equiv \tau_D\,(1 + 2L_2^2/l_0^2)$, and $\tau'_{D3} \equiv \tau_D(1 + 2L_3^2/l_0^2)$. The calculation sketched above yields the following expressions for B_1 and B_2:

$$\begin{aligned} B_1(\boldsymbol{k}, t, d = 3) = {} & \frac{\pi^{1/2}}{2}\frac{\tau_D}{v(\boldsymbol{k})}\,\{\mathrm{erf}(v(\boldsymbol{k})\,(t/\tau_D)\;T_2(t)^{-1/2}) \\ & - \exp(v(\boldsymbol{k})^2)[\mathrm{erf}(v(\boldsymbol{k})) - \mathrm{erf}(v(\boldsymbol{k})\;T_1(t)\;T_2(t)^{-1/2})]\}, \\ B_2(\boldsymbol{k}, t, d = 3) = {} & \frac{\pi^{1/2}}{2}\frac{\tau'_{D1}}{v_1(\boldsymbol{k})}\;\theta_4^2(t)^{-1/2}\;\theta_4^3(t)^{-1/2}\;\{\mathrm{erf}(v_1(\boldsymbol{k})\,(t/\tau'_{D1})\;\theta_2^1(t)^{-1/2}) \\ & - \exp\{v_1(\boldsymbol{k})^2\,\theta_4^1(t)\}[\mathrm{erf}(v_1(\boldsymbol{k})\,\theta_4^1(t)^{1/2}) - \mathrm{erf}(v_1(\boldsymbol{k})\,\theta_3^1(t)\,\theta_2^1(t)^{-1/2})]\}, \end{aligned}$$

with

$$\begin{aligned} \boldsymbol{N}_1(\boldsymbol{k}) &\equiv (\boldsymbol{e}_1 + 2\mathrm{i}\boldsymbol{k}\;l_0\,\epsilon)\,(2\,(D/\,\overline{u}\,l_1)^2)^{-1/2}, \\ v_1(\boldsymbol{k}) &\equiv (\boldsymbol{N}_1^2(\boldsymbol{k}))^{1/2}, \\ \theta_m^j(t) &\equiv 1 + m\,t/\tau'_{Dj} \quad \text{with} \quad m = 1, 2, 3, 4 \quad \text{and} \quad j = 1, 2, 3 \end{aligned}$$

and $T_m(t)$, $v(\boldsymbol{k})$ as defined in Appendix B.

REFERENCES

Abramowitz, M. & Stegun, I. A. 1972 *Handbook of Mathematical Functions.* Dover.

Attinger, S. 1997 Die zeitliche Entwicklung von Transportparametern in einem chemisch heterogenen Medium. PhD thesis, University of Heidelberg.

Batchelor, G. K. 1949 Diffusion in a field of homogeneous turbulence I, eulerian analysis. *Austral. J. Sci. Res.* **2**, 437–450.

Batchelor, G. K. 1952 Diffusion in a field of homogeneous turbulence II, the relative motion of particles. *Proc. Camb. Phil. Soc.* **48**, 345–362.

Bellin, A., Rinaldo, A., Bosma W. J. P., Zee, S. E. A. T. M. van der & Rubin, Y. 1993 Linear equilibrium adsorbing solute transport in physically and chemically heterogeneous porous formations 1. Analytical solutions. *Water Resour. Res.* **29**, 4019–4013.

Bouchaud, J. P. & Georges, A. 1990 Anomalous diffusion in disordered media: Statistical mechanisms, models and physical applications. *Phys. Rep.* **195**, 127–293.

Burr, D. T., Sudicky, E. A. & Naff, R. L. 1994 Nonreactive and reactive solute transport in three-dimensional heterogeneous porous media: Mean displacement, plume spreading, and uncertainty. *Water Resour. Res.* **30**, 791–815.

Chrysikopoulos, C., Kitanidis, P. K. & Roberts, P. V. 1990 Analysis of one-dimensional solute transport through porous media with spatially variable retardation factor. *Water Resour. Res.* **26**, 437–446.

Dagan, G. 1984 Solute transport in heterogeneous porous formations. *J. Fluid Mech.* **145**, 151–177.

Dagan, G. 1988 Time-dependent macrodispersion for solute transport in anisotropic heterogeneous aquifers. *Water Resour. Res.* **24**, 1491–1500.

Dagan, G. 1989 *Flow and Transport in Porous Formations.* Springer.

Dagan, G. 1990 Transport in heterogeneous porous formations: Spatial moments, ergodicity, and effective dispersion. *Water Resour. Res.* **26**, 1281–1290.

Dagan, G. 1991 Dispersion of a passive solute in non-ergodic transport by steady velocity fields in heterogeneous formations. *J. Fluid Mech.* **233**, 197–210.

Dentz, M. 1997 Zeitverhalten von Transportkoeffizienten in heterogenen porösen Medien. Diploma Thesis, University of Heidelberg.

Dentz, M., Attinger, S., Kinzelbach, H. & Kinzelbach, W. 1998 Temporal behaviour of a solute cloud in a heterogeneous porous medium. *Water Resour. Res.* (submitted).

Dentz, M. & Kinzelbach, H. 1998 Technical note on the paper 'On the influence of pore-scale dispersion in nonergodic transport in heterogeneous formations' by A. Fiori. *Transport in Porous Media* (to appear).

Fiori, A. 1996 Finite Pecelt extensions of Dagan's solutions to transport in anisotropic heterogeneous formations. *Water Resour. Res.* **32**, 193–198.

Fiori, A. 1998 On the influence of the pore-scale dispersion in nonergodic transport in heterogeneous formations. *Transport in Porous Media* **30**, 57–73.

Garabedian, S. P., Gelhar, L. W. & Celia, M. A. 1988 Large scale dispersivity transport in aquifers: Field experiments and reactive transport theory. *Rep.* 315. Parsons Lab., MIT Cambridge, USA.

Gelhar, L. W. 1993 *Stochastic Subsurface Hydrology*. Prentice Hall.

Gelhar, L. W. & Axness, C. L. 1983 Three-dimensional analysis of macrodispersion in aquifers. *Water Resour. Res.* **19**, 161–180.

Gradshteyn, I. S. & Ryzhik, I. M. 1980 *Table of Integrals, Series, and Products*. Academic.

Haus, J. W. & Kehr, K. W. 1987 Diffusion in regular and disordered lattices. *Phys. Rep.* **150**, 263–406.

Kabala, Z. J. & Sposito, G. 1991 Stochastic model of reactive solute transport with time varying velocity in a heterogeneous aquifer. *Water Resour. Res.* **27**, 341–350.

Kapoor, V. & Kitanidis, P. K. 1996 Concentration fluctuations and dilution in two-dimensionally periodic heterogeneous porous media. *Transport in Porous Media* **21**, 91–119.

Karickhoff, S. W., Brown, D. S. & Scott, T. A. 1979 Sorption of hydrophobic pollutants on natural sediments. *Water Resour. Res.* **13**, 241–248.

Kitanidis, P. K. 1988 Prediction by the method of moments of transport in a heterogeneous formation. *J. Hydrology* **102**, 453–473.

Kitanidis, P. K. 1992 Analysis of macrodispersion through volume averaging: Moment equations. *Stochastic Hydrology and Hydraulics* **6**, 5–25.

Metzger, D., Kinzelbach, H. & Kinzelbach, W. 1996 Effective dispersion of a solute cloud in a chemically heterogeneous porous medium: comparison of two ensemble-averaging procedures. *Water Resour. Res.* **32**, 3311–3319.

Metzger, D., Kinzelbach, H. & Kinzelbach, W. 1998 Asymptotic transport parameters in a heterogeneous porous medium. *Stochastic Hydrology and Hydraulics* (to appear).

Miralles-Wilhelm, F. & Gelhar, L. W. 1996 Stochastic analysis of sorption macrokinetics in heterogeneous aquifers. *Water Resour. Res.* **32**, 1541–1549.

Naff, R. L. 1990 On the nature of the dispersive flux in saturated heterogeneous porous media. *Water Resour. Res.* **26**, 1013–1026.

Rajaram, H. & Gelhar, L. W. 1993 Plume scale-dependent dispersion in heterogeneous aquifers. *Water Resour. Res.* **29**, 3249–3276.

Roberts, P. V., Goltz, M. N. & Mackay, D. M. 1986 A natural gradient experiment on solute transport in a sand aquifer, 3. retardation estimates and mass balances for organic solutes. *Water Resour. Res.* **22**, 2047–2058.

Shvidler, M. I. 1993 Correlation model of transport in random fields. *Water Resour. Res.* **29**, 3189–3199.